# NATIONAL ADVISORY COMMITTEE FOR AERONAUTICS

**TECHNICAL NOTE 4103**

## IMPACT-LOADS INVESTIGATION OF CHINE-IMMERSED MODEL HAVING A CIRCULAR-ARC TRANSVERSE SHAPE

By Philip M. Edge, Jr.

Langley Aeronautical Laboratory
Langley Field, Va.


Washington
September 1957

NATIONAL ADVISORY COMMITTEE FOR AERONAUTICS

TECHNICAL NOTE 4103

# IMPACT-LOADS INVESTIGATION OF CHINE-IMMERSED MODEL HAVING A CIRCULAR-ARC TRANSVERSE SHAPE

By Philip M. Edge, Jr.

## SUMMARY

An investigation of hydrodynamic impact loads on chine-immersed bodies of heavy beam loading at the Langley impact basin has been expanded to include transversely curved models in addition to models of prismatic shape. This paper presents the results from tests of a chine-immersed model having a circular-arc cross section with a radius of 1 beam. The results were obtained from fixed-trim impacts made in smooth water over a wide range of trim and initial flight-path angles. Most of the impacts were made at a beam-loading coefficient of 18.59 with a few impacts at beam-loading coefficients of 27.59 and 36.57.

The data are presented in tables, and the coefficients of loads and motion are presented in figures as a function of trim and initial flight-path angles. The circular-arc model experienced loads greater than loads predicted by theory for this configuration by about 10 percent. These loads are as much as 12 percent less than the loads measured under similar conditions for a model with concave-convex cross section with a similar effective angle of dead rise.

## INTRODUCTION

Investigations of hydrodynamic impact loads on chine-immersed bodies at the Langley impact basin have dealt largely with models of flat and V-bottom transverse shapes such as reported in references 1 and 2. This study was expanded in reference 3 to a model with a concave-convex transverse shape (a constant-force-type bottom). The concave-convex model yielded maximum loads comparable to loads predicted by theory for a V-bottom of the same effective dead-rise angle and indicated that such shape deviations from the conventional V-bottom have little effect on the maximum load. Further studies of the effect of transverse shape on hydrodynamic impact loads, with greater deviations from the V-configuration, were made on a model of circular-arc cross section having a radius of 1 beam. This bottom shape was installed on a model having a straight keel, and a series of fixed-trim impacts in smooth water was made at the Langley impact basin. Most of these impacts were made at a beam-loading

coefficient of 18.59 and covered a range of trim and initial flight-path angles; however, a few impacts were made at a trim angle of 8° with beam-loading coefficients of 27.59 and 36.57. The purpose of this investigation was to obtain loads and moment data on a chine-immersed model having a circular-arc transverse shape.

This report tabulates the basic data of the investigation, presents the various coefficients as variations with trim and initial flight-path angles, and compares the maximum loads obtained with loads predicted for this model by the theory of reference 4. This theory is used to indicate the relationship of the loads predicted for the circular-arc model and the loads predicted for a V-bottom model. Additional comparisons are made herein of the maximum loads for the circular-arc model and the maximum loads for the concave-convex model of reference 3.

## SYMBOLS

| | |
|---|---|
| $\gamma$ | flight-path angle relative to undisturbed water surface, deg |
| $\rho$ | mass density of water, 1.938 slugs/cu ft |
| $\tau$ | trim angle, deg |
| $b$ | model beam, ft |
| $g$ | acceleration due to gravity, 32.2 ft/sec$^2$ |
| $t$ | time after contact, sec |
| $W$ | dropping weight, lb |
| $n_i$ | impact load factor normal to undisturbed water surface, $\frac{F_V}{W}$ |
| $\dot{x}$ | velocity of model parallel to undisturbed water surface, ft/sec |
| $z$ | draft of model normal to undisturbed water surface, ft |
| $\dot{z}$ | velocity of model normal to undisturbed water surface, ft/sec |
| $M_Y$ | pitching moment about step, lb-ft |
| $F_n$ | hydrodynamic force normal to keel, lb |
| $V$ | resultant velocity of model, ft/sec |

$F_v$ vertical component of hydrodynamic force, lb

$C_L$ impact lift coefficient, $\frac{n_i W}{\frac{1}{2}\rho V_o^2 b^2} = \frac{F_v}{\frac{1}{2}\rho V_o^2 b^2}$

$C_d$ draft coefficient, $\frac{z}{b}$

$C_V$ vertical-velocity coefficient, $\frac{\dot{z}}{\dot{z}_o}$

$C_t$ time coefficient, $\frac{V_o t}{b}$

$C_{cp}$ center-of-pressure coefficient, $\frac{\text{Center of pressure measured from step}}{b}$

$C_m$ pitching-moment coefficient, $\frac{M_Y}{\frac{1}{2}\rho V_o^2 b^3}$

$C_\Delta$ beam-loading coefficient, $\frac{W}{\rho g b^3}$

Subscripts:

o instant of initial contact with water surface

s referred to step (stern of model)

max maximum

## APPARATUS

Tests were made in the Langley impact basin with the same equipment described in reference 5. This equipment consists of a catapult, a testing carriage to which the model is attached, associated instrumentation for measuring loads and motions of the model, and an arresting gear. The model is attached to the carriage at all times by a boom mounted on a parallel linkage which permits the model to move freely relative to the carriage in the vertical direction.

## Model

The bottom of the model tested had a circular-arc cross section with a radius of 1 beam as shown in figure 1. The effective dead-rise angle along this arc is 15°. The model had a beam of 1 foot and a straight-keel profile 12 feet long with an arbitrarily curved nose section 1 foot long. The basic model was of light sheet-metal construction with a bottom of wood covered with fiber glass. As shown in figure 2, the model was attached rigidly to the carriage boom through a load-measuring dynamometer and was held fixed in trim throughout the impact by this mounting.

## Instrumentation

The instrumentation consisted of a multichannel oscillograph, accelerometers, a dynamometer, water-contact indicator, and electrical pickups for measuring displacements and velocities. All measurements were recorded on the oscillograph along with 0.01-second timing.

Accelerations in the vertical direction were measured by oil-damped unbonded strain-gage-type accelerometers having undamped natural frequencies of 17 and 120 cycles per second. Extraneous structural vibrations were eliminated by electrical fairing. Loads normal to the keel of the model $F_n$ and pitching moments about the forward attachment point were obtained from the strain-gage dynamometer mounted between the model and the supporting carriage boom. These measurements were corrected for the distribution of mass and center of gravity of the parts located below the dynamometer, and the pitching moments were referred to the step $M_Y$. Only these corrected values and moments about the step are presented. The initial contact of the model with the water and the rebound of the model from the water were determined by means of an electrical circuit completed by the water. Horizontal velocity was computed from photoelectric-cell measurements of horizontal displacement. Vertical-displacement measurements were obtained from a slide-wire, and vertical velocity was obtained by an induction-type generator driven by the carriage boom.

## TEST PROCEDURE

This investigation consisted of a series of impacts in smooth water at fixed trim angles from 0° to 30° and at initial flight-path angles from approximately 3° to 20°. At a beam-loading coefficient of 18.59, impacts were made at trim angles of 0°, 4°, 8°, 12°, 15°, 20°, and 30°; whereas at beam-loading coefficients of 27.59 and 36.57, impacts were made at a trim angle of 8° only. The flight-path angles were varied at all trim angles

except 0° where the impacts were limited to vertical drop without forward speed ($\gamma_o = 90°$). These impacts without forward speed were made over a range of vertical velocities varying from about 3 feet per second to approximately 11.5 feet per second. The forward-speed impacts ranged in vertical velocity from approximately 4 feet per second to approximately 11 feet per second and ranged in horizontal velocity from 20 feet per second to over 88 feet per second. Throughout the immersion a lift force equal to the total weight of the model and drop linkage was applied to the model to simulate wing lift as described in reference 5.

Several times during the investigation, repeat impacts were made with the test conditions as nearly the same as possible as a check on the consistency of the test equipment. The data obtained from these impacts showed that no significant performance changes occurred during the investigation. Only the average values of these data are presented.

## RESULTS AND DISCUSSION

The experimental data obtained in this investigation are presented in table I for each of the impacts made. This table shows the measured values of loads and motions at contact with the water, at maximum acceleration, at maximum draft, and at rebound. In addition to these measured quantities, the computed values of lift coefficient and pitching-moment coefficient at $n_{1,max}$ are given.

Sample time histories, which illustrate typical variations of the data obtained throughout the impacts at $C_\Delta = 18.59$, are presented in figures 3 to 5. The variations of impact load factor, draft, vertical velocity, and pitching moment with time are shown in figure 3 for impacts without forward speed for three vertical velocities. The vertical load and pitching moment for two of these drop tests are shown as time histories in coefficient form in figure 4. Figure 5 presents the vertical-load, draft, vertical-velocity, center-of-pressure, and pitching-moment time histories in coefficient form for three flight-path angles at each of three trim angles ($\tau = 4°$, 8°, and 30°). The time histories of figures 3 and 4 show that, for the flat impact of a vertical drop at a trim angle of 0°, the load and pitching moment build up rapidly on the circular-arc bottom at a beam-loading coefficient of 18.59. Although the small velocities of the impacts without forward speed are not well expressed in coefficient form, the loads and moments in this form are useful for comparison with forward-speed impact conditions. The loads and moments of figures 4 and 5 show that, as the flat impact at the zero trim angle of the vertical drop without forward speed ($\gamma = 90°$) is departed from and the more realistic smooth-water landing conditions with significant trim are approached, the load during an impact process is applied more gradually and is less severe in magnitude. The gradual application of the hydrodynamic impact load

results in a flatness of the impact-lift-coefficient peak. Since this flat peak may extend over several hundredths of a second, the instant of peak or maximum load could not be sharply defined; thus, the values of other parameters read at this instant (draft, vertical velocity, and pitching moment) for this type of impact were not reliable.

In figure 6 sample time histories of the coefficients obtained for impacts at a trim angle of 8° for beam-loading coefficients of 18.59 and 36.57 are compared. Other than the magnitude of the values, the general appearance and characteristics of the time histories are similar for each beam loading.

In figure 7 the variations of load, draft, vertical-velocity, time, pitching-moment, and center-of-pressure coefficients with initial flight-path angle are shown for three trim angles at $C_{\Delta} = 18.59$. In figure 8 comparisons are made of the variations shown in figure 7 for $C_{\Delta} = 18.59$ and variations obtained for $C_{\Delta} = 36.57$ at a trim angle of 8°. The variations shown in figures 7 and 8 indicate that, in general, separate relationships exist for each trim angle and for each value of beam-loading coefficient. Exceptions to this observation are indicated in figure 8(c) where vertical velocity at rebound is apparently independent of beam loading and in figure 7(b) where maximum draft is largely independent of trim angle.

The experimental variations of lift and draft coefficients with trim angle are shown in figure 9 for four initial flight-path angles at $C_{\Delta} = 18.59$. The variations shown are orderly and in line with what is expected for the range of parameters involved. In addition to presenting the variations of the coefficients with trim for typical flight-path angles, this figure represents a summary of the experimental data from which cross plots may be obtained for predicting coefficients at any trim or flight-path angle within the range tested.

## Comparison of Calculation and Experiment

Maximum lift coefficients for the circular-arc model were calculated for comparison with the experimental results obtained in this investigation. Also maximum lift coefficients for a V-bottom model were calculated to show the relations of the circular-arc loads to loads computed for a V-bottom model with the same effective dead-rise angle, 15° (as defined in fig. 1). These calculations were made by using the theory of reference 4 as well as planing data of reference 6, which were for the same circular-arc cross section.

The variations of the maximum loads with angle of trim are shown in figure 10 for three initial flight-path angles ($\gamma_o = 5.5°$, 10°, and 20°)

over a range of trim angles ($\tau$ = 4° to 20°) for a beam-loading coefficient of 18.59. In general, the calculated loads are similar to but lower than the experimental loads. At low flight-path angles with appreciable trim angles (conditions which correspond to smooth-water or very mild rough-water impacts) the maximum loads from calculation and experiment are in close agreement considering the low values of lift coefficient and the accuracies involved. Although no one theory accurately predicts the maximum loads over the entire range shown, the general trend of the maximum lift coefficient appears well represented by the variation calculated for the circular-arc cross section. If the loads calculated for a V-bottom of the effective dead-rise angle are used, the prediction is conservative in the region of low trim angle and high flight-path angle where the loads are most critical and is nonconservative in the region of high trim and high flight-path angle where the loads are less critical. From the comparisons shown in figure 10, the conclusion is made that, for a beam-loading coefficient of 18.59, calculations for the circular-arc shape when increased by about 10 percent would provide the best estimate of the maximum loads for the circular-arc transverse shape tested.

In figure 11 the effect of beam loading is considered for the one trim angle ($\tau$ = 8°) where experimental data were obtained at higher beam loadings. Maximum loads obtained at $C_{\Delta}$ = 18.59 and 36.57 are compared with loads predicted by theory for the circular-arc cross section. The loads obtained experimentally over the flight-path-angle range are greater than those predicted by theory for the circular-arc shape by about the same amount for both beam loadings.

## Experimental Comparison With Concave-Convex Model

The experimental variations of the maximum lift coefficient with trim angle for the circular-arc model are compared in figure 12 with the experimental variation presented in reference 3 for the concave-convex bottom. Experimental variations are presented in this figure for initial flight-path angles of 5.5°, 10°, 15°, and 20°. The comparisons shown indicate that the maximum loads on the circular-arc bottom range from a few percent less than maximum loads on the concave-convex model at 6° trim to an average of over 12 percent less at trims above 15° except at the flight-path angle of 5.5° where the absolute differences in lift coefficient are small.

## Observations on Effect of Transverse Curvature

In reference 3 maximum loads on a model having concave-convex transverse curvature were, in general, similar to the maximum loads predicted for a V-bottom of the average dead-rise angle. These results implied that the V transverse shape of a chine-immersed model can be

altered somewhat without significant change in maximum loads during hydrodynamic impact. These observations were based on comparisons of experimental data for the concave-convex model with loads predicted by theory as no experimental data are available for V-bottoms of the corresponding average dead-rise angle. Inasmuch as the data of the present investigation were obtained from a model of nearly the same average dead-rise angle and with convex curvature only, additional observations can be made as to the effect of transverse curvature on maximum loads. Comparisons of the maximum loads of this investigation and of reference 3 have shown that the circular-arc model experiences maximum loads which are less by 12 percent than those of the concave-convex model. Since the transverse shapes of both models are similar in the keel region, the differences in dead-rise slope near the chine appear to have a significant effect on the magnitude of the loads during an impact process. Furthermore, the effect of the dead-rise angle at the chine is evidently of more importance at high angles of trim.

## CONCLUSIONS

An analysis of experimental data obtained in an impact-basin investigation of a chine-immersed model having a circular-arc transverse shape of 1-beam radius leads to the following conclusions:

1. The data indicated that the impact loads varied from rapidly applied sharp peak loads for the flat impacts of the drops without forward speed to very gradually applied loads whose peaks endured several hundredths of a second for more realistic smooth-water landing conditions (impacts with significant trim and low flight-path angles).

2. For the trim-angle and flight-path-angle range tested, the maximum loads can be estimated by increasing the calculated loads by 10 percent for this circular-arc configuration.

3. Over the ranges of trim angles and flight-path angles tested, the maximum loads predicted from calculations of a V-bottom of the effective dead-rise angle ($15^\circ$) of the circular arc are conservative in the region of low trim and high flight-path angle and are nonconservative in the region of high trim and high flight-path angle.

4. The experimental maximum loads of the circular-arc model were as much as 12 percent less than the maximum loads measured on a concave-convex model. The results indicate that the transverse shape of the bottom at the chine is of primary importance for forward speed impacts with significant trim.

Langley Aeronautical Laboratory,
National Advisory Committee for Aeronautics,
Langley Field, Va., June 12, 1957.

## REFERENCES

1. McArver, A. Ethelda: Water-Landing Investigation of a Model Having Heavy Beam Loadings and 0° Angle of Dead Rise. NACA TN 2330, 1951.

2. Batterson, Sidney A., and McArver, A. Ethelda: Water Landing Investigation of a Model Having a Heavy Beam Loading and a 30° Angle of Dead Rise. NACA TN 2015, 1950.

3. Edge, Philip M., Jr.: Impact-Loads Investigation of Chine-Immersed Models Having Concave-Convex Transverse Shape and Straight or Curved Keel Lines. NACA TN 3940, 1957.

4. Schnitzer, Emanuel: Theory and Procedure for Determining Loads and Motions in Chine-Immersed Hydrodynamic Impacts of Prismatic Bodies. NACA Rep. 1152, 1953. (Supersedes NACA TN 2813.)

5. Batterson, Sidney A.: The NACA Impact Basin and Water Landing Tests of a Float Model at Various Velocities and Weights. NACA Rep. 795, 1944. (Supersedes NACA WR L-163.)

6. Wadlin, Kenneth L., and McGehee, John R.: Planing Characteristics of Three Surfaces Representative of Hydro-Ski Forms. NACA RM L9C03, 1949.

TABLE I.- IMPACT-LOADS DATA FROM TESTS OF A NARROW BEAM MODEL OF CIRCULAR-ARC TRANSVERSE SHAPE

| Run | Trim, deg | At contact | | | At $n_{I,max}$ | | | | | | | | At $z_{max}$ | | | At rebound | |
|---|---|---|---|---|---|---|---|---|---|---|---|---|---|---|---|---|---|
| | | $\dot{z}_o$, ft/sec | $\dot{x}_o$, ft/sec | $\gamma_o$, deg | t, sec | $n_I$, g | $F_n$, lb | z, ft | $\dot{z}$, ft/sec | $M_Y$, lb-ft | $C_L$ | $C_{m,s}$ | t, sec | $n_I$, g | z, ft | t, sec | $\dot{z}$, ft/sec |
| $C_\Delta$ = 18.59 | | | | | | | | | | | | | | | | | |
| 1 | 0 | 3.30 | 0 | 90 | 0.027 | 0.78 | 696 | 0.104 | 2.86 | 3,250 | 85.43 | 308.02 | 0.426 | 0.12 | 0.648 | ----- | ----- |
| 2 | | 4.44 | | | .030 | 1.35 | 1160 | .129 | 3.78 | 5,670 | 82.05 | 296.86 | .426 | .30 | .813 | ----- | ----- |
| 3 | | 5.02 | | | .025 | 1.62 | 1437 | .114 | 4.22 | 7,524 | 77.00 | 308.11 | .426 | .24 | .902 | ----- | ----- |
| 4 | | 5.72 | | | .012 | 1.96 | 1079 | .071 | 5.32 | 6,445 | 71.77 | 203.24 | .435 | .36 | 1.068 | ----- | ----- |
| 5 | | 6.91 | | | .012 | 3.17 | 1799 | .080 | 6.29 | 10,600 | 79.35 | 229.08 | .422 | .39 | 1.214 | ----- | ----- |
| 6 | | 8.01 | | | .012 | 3.99 | 2345 | .101 | 7.22 | 14,030 | 74.50 | 225.67 | .437 | .41 | 1.214 | ----- | ----- |
| 7 | | 9.68 | | | .011 | 5.65 | 3486 | .108 | 8.76 | 20,951 | 72.19 | 230.74 | .440 | .18 | 1.644 | ----- | ----- |
| 8 | | 11.48 | | | .012 | 5.89 | 4009 | .135 | 10.12 | 23,560 | 53.48 | 182.93 | .462 | .44 | 1.948 | ----- | ----- |
| 9 | 4 | 4.71 | 87.72 | 3.07 | 0.073 | 1.03 | 1330 | 0.286 | 2.42 | 2,572 | 0.16 | 0.35 | 0.174 | 0.62 | 0.396 | 0.491 | -1.23 |
| 10 | | 8.10 | 77.52 | 5.96 | .070 | 1.76 | 2165 | .467 | 4.62 | 5,763 | .35 | .98 | .211 | .54 | .738 | .661 | -1.58 |
| 11 | | 10.30 | 59.00 | 9.90 | .069 | 2.08 | 2467 | .593 | 6.73 | 8,257 | .69 | 2.38 | .268 | .59 | 1.083 | 1.079 | -.48 |
| 12 | | 10.21 | 51.55 | 11.20 | .062 | 2.06 | 2360 | .550 | 6.86 | 7,413 | .89 | 2.77 | .290 | .44 | 1.134 | 1.085 | -1.01 |
| 13 | | 10.16 | 40.65 | 14.03 | .063 | 1.84 | 2086 | .562 | 7.26 | 6,625 | 1.25 | 3.89 | .348 | .41 | 1.334 | ----- | ----- |
| 14 | | 10.60 | 29.07 | 20.03 | .065 | 1.71 | 1990 | .615 | 7.70 | 7,761 | 2.14 | 8.37 | .400 | .38 | 1.561 | ----- | ----- |
| 15 | 8 | 4.66 | 88.50 | 3.01 | 0.087 | 1.34 | 1676 | 0.317 | 1.58 | 3,040 | 0.20 | 0.40 | 0.137 | 1.02 | 0.350 | 0.331 | -2.55 |
| 16 | | 4.80 | 77.52 | 3.55 | .086 | 1.14 | 1408 | .313 | 2.33 | 2,265 | .23 | .39 | .146 | .93 | .378 | .376 | -2.20 |
| 17 | | 8.62 | 66.67 | 7.37 | .080 | 1.82 | 2276 | .572 | 4.62 | 5,433 | .48 | 1.24 | .199 | .83 | .842 | .559 | -2.99 |
| 18 | | 8.36 | 60.61 | 7.85 | .071 | 1.68 | 2002 | .504 | 4.93 | 4,611 | .54 | 1.27 | .216 | .72 | .814 | .590 | -2.95 |
| (a) | | 9.33 | 60.61 | 8.73 | .077 | 1.78 | 2463 | .612 | 5.81 | 6,419 | .57 | 1.76 | .227 | .82 | .990 | .659 | -2.68 |
| 19 | | 9.33 | 53.19 | 9.96 | .079 | 1.66 | 2031 | .615 | 5.76 | 5,173 | .68 | 1.83 | .264 | .63 | 1.073 | .804 | -1.98 |
| 20 | | 8.62 | 41.67 | 11.69 | .071 | 1.33 | 1571 | .522 | 5.85 | 3,389 | .88 | 2.16 | .298 | .41 | 1.066 | .932 | -1.89 |
| 21 | | 9.33 | 40.82 | 12.87 | .077 | 1.41 | 1768 | .630 | 6.60 | 4,157 | .96 | 2.45 | .322 | .48 | 1.275 | 1.046 | -1.54 |
| 22 | | 10.78 | 41.67 | 14.50 | .070 | 1.71 | 2092 | .633 | 7.35 | 5,740 | 1.10 | 3.14 | .290 | .56 | 1.282 | .922 | -2.42 |
| 23 | | 9.24 | 31.65 | 16.27 | .071 | 1.20 | 1468 | .609 | 7.17 | 2,487 | 1.32 | 2.83 | .381 | .37 | 1.494 | 1.146 | -.44 |
| 24 | | 10.78 | 33.11 | 18.03 | .072 | 1.52 | 1819 | .685 | 7.66 | 4,204 | 1.50 | 3.58 | .374 | .39 | 1.574 | 1.164 | -1.32 |
| 25 | | 9.90 | 25.97 | 20.87 | .079 | 1.24 | 1472 | .707 | 7.44 | 3,706 | 1.91 | 4.95 | .422 | .34 | 1.712 | ----- | ----- |
| 26 | 12 | 4.75 | 87.72 | 3.10 | 0.086 | 1.54 | 2050 | 0.307 | 1.36 | 2,638 | 0.24 | 0.35 | 0.130 | 1.23 | 0.341 | 0.276 | -3.08 |
| 27 | | 8.27 | 78.13 | 6.04 | .083 | 2.10 | 2697 | .550 | 3.65 | 4,944 | .41 | .83 | .151 | 1.61 | .667 | .370 | -4.49 |
| 28 | | 10.60 | 66.23 | 9.09 | .080 | 2.27 | 2854 | .688 | 5.85 | 5,905 | .60 | 1.35 | .185 | 1.29 | .962 | .490 | -4.27 |
| 29 | | 10.43 | 53.76 | 10.98 | .082 | 1.92 | 2339 | .747 | 6.29 | 4,241 | .77 | 1.81 | .231 | 1.01 | 1.180 | .631 | -3.96 |
| 30 | | 10.69 | 36.36 | 16.38 | .082 | 1.51 | 1878 | .781 | 7.66 | 4,644 | 1.26 | 3.34 | .317 | .60 | 1.540 | .905 | -2.42 |
| 31 | | 10.91 | 27.47 | 21.66 | .084 | 1.24 | 1509 | .817 | 8.36 | 3,818 | 1.69 | 4.51 | .419 | .38 | 1.865 | 1.191 | -1.06 |
| 32 | 15 | 5.15 | 89.29 | 3.30 | 0.090 | 1.68 | 2300 | 0.369 | 1.36 | 2,891 | 0.25 | 0.37 | 0.121 | 1.53 | 0.375 | 0.272 | -3.56 |
| 33 | | 9.06 | 79.68 | 6.49 | .087 | 2.29 | 2971 | .661 | 3.92 | 4,861 | .43 | .78 | .143 | 1.77 | .704 | .343 | -5.32 |
| 34 | | 10.82 | 66.67 | 9.22 | .087 | 2.45 | 3147 | .774 | 5.46 | 6,483 | .64 | 1.47 | .172 | 1.71 | .996 | .434 | -5.37 |
| 35 | | 10.65 | 44.05 | 13.59 | .086 | 1.72 | 2099 | .796 | 7.04 | 4,513 | 1.00 | 2.27 | .256 | .89 | 1.331 | .729 | -3.48 |
| 36 | | 10.47 | 42.02 | 13.99 | .086 | 1.58 | 2052 | .796 | 7.26 | 4,484 | 1.01 | 2.47 | .269 | .82 | 1.368 | .749 | -3.74 |
| 37 | | 11.04 | 37.88 | 16.25 | .089 | 1.50 | 1887 | .857 | 7.48 | 4,597 | 1.16 | 3.05 | .296 | .70 | 1.521 | .865 | -3.21 |
| 38 | | 10.82 | 33.22 | 18.04 | .087 | 1.44 | 1812 | .848 | 7.44 | 4,534 | 1.41 | 3.83 | .325 | .62 | 1.623 | 1.018 | -2.77 |
| 39 | | 10.52 | 24.88 | 22.92 | .087 | 1.13 | 1353 | .842 | 8.01 | 3,077 | 1.86 | 4.35 | .413 | .45 | 1.948 | 1.562 | -.75 |
| 40 | 20 | 3.92 | 78.13 | 2.87 | 0.097 | 1.23 | 1717 | 0.267 | 1.06 | 1,719 | 0.24 | 0.29 | 0.116 | 1.22 | 0.283 | 0.261 | -3.12 |
| 41 | | 6.42 | 53.48 | 6.85 | .096 | 1.19 | 1594 | .504 | 3.56 | 2,496 | .49 | .89 | .191 | 1.02 | .667 | .440 | -3.87 |
| 42 | | 7.61 | 42.19 | 10.22 | .096 | 1.06 | 1379 | .630 | 5.19 | 2,239 | .69 | 1.26 | .251 | .84 | .999 | .626 | -3.65 |
| 43 | | 10.52 | 45.25 | 13.09 | .090 | 1.62 | 2137 | .811 | 6.51 | 3,806 | .90 | 1.82 | .233 | 1.11 | 1.263 | .618 | -4.88 |
| 44 | | 10.52 | 37.04 | 15.86 | .095 | 1.37 | 1768 | .867 | 7.08 | 3,389 | 1.11 | 2.36 | .299 | .76 | 1.506 | .817 | -3.65 |
| 45 | | 10.60 | 25.51 | 22.56 | .150 | 1.07 | 1391 | 1.162 | 6.20 | 3,397 | 1.67 | 4.59 | .415 | .53 | 2.025 | 1.428 | -1.67 |
| 46 | 30 | 3.92 | 73.76 | 2.96 | 0.111 | 1.30 | 1931 | 0.261 | 0.26 | 2,532 | 0.27 | 0.45 | 0.115 | 1.30 | 0.267 | 0.251 | -2.82 |
| 47 | | 7.79 | 59.70 | 7.43 | .115 | 1.65 | 2307 | .698 | 3.08 | 3,781 | .54 | 1.08 | .175 | 1.51 | .802 | .399 | -5.46 |
| 48 | | 10.38 | 51.55 | 11.39 | .104 | 1.85 | 2541 | .925 | 5.32 | 4,515 | .80 | 1.69 | .199 | 1.53 | 1.162 | .478 | -5.94 |
| 49 | | 10.43 | 39.68 | 14.73 | .150 | 1.52 | 2232 | 1.183 | 4.31 | 4,234 | 1.08 | 2.60 | .256 | 1.10 | 1.395 | .651 | -4.84 |
| 50 | | 10.52 | 30.21 | 19.20 | .156 | 1.20 | 1735 | 1.337 | 5.46 | 3,649 | 1.40 | 3.68 | .341 | .69 | 1.789 | .964 | -3.34 |
| $C_\Delta$ = 27.59 | | | | | | | | | | | | | | | | | |
| 51 | 8 | 4.62 | 84.75 | 3.12 | 0.095 | 0.84 | 1618 | 0.350 | 2.51 | 2,692 | 0.21 | 0.39 | 0.180 | 0.72 | 0.461 | 0.460 | -2.11 |
| 52 | | 8.32 | 76.34 | 6.22 | .081 | 1.45 | 2711 | .599 | 5.10 | 5,848 | .44 | 1.02 | .238 | .79 | .990 | .603 | -3.70 |
| 53 | | 10.69 | 51.28 | 11.78 | .079 | 1.50 | 2786 | .733 | 7.48 | 7,876 | .97 | 2.96 | .329 | .54 | 1.531 | 1.000 | -2.64 |
| 54 | | 10.69 | 43.29 | 13.87 | .080 | 1.39 | 2442 | .811 | 7.74 | 8,017 | 1.24 | 4.16 | .367 | .44 | 1.690 | 1.148 | -2.11 |
| 55 | | 10.78 | 31.55 | 18.86 | .089 | 1.06 | 1840 | .861 | 8.36 | 6,725 | 1.70 | 6.24 | .489 | .30 | 2.173 | 1.582 | -1.32 |
| $C_\Delta$ = 36.57 | | | | | | | | | | | | | | | | | |
| 56 | 8 | 4.71 | 86.21 | 3.13 | 0.096 | 0.80 | 1908 | 0.378 | 2.68 | 3,950 | 0.25 | 0.55 | 0.221 | 0.53 | 0.544 | 0.536 | -2.89 |
| 57 | | 9.02 | 73.26 | 7.02 | .083 | 1.24 | 2992 | .670 | 6.03 | 7,591 | .54 | 1.44 | .295 | .65 | 1.257 | .795 | -2.99 |
| 58 | | 10.96 | 55.56 | 11.16 | .083 | 1.38 | 3295 | .836 | 8.23 | 10,481 | 1.01 | 3.37 | .347 | .49 | 1.749 | 1.132 | -2.02 |
| 59 | | 11.00 | 45.66 | 13.55 | .085 | 1.20 | 2784 | .836 | 8.49 | 8,945 | 1.29 | 4.18 | .436 | .32 | 2.004 | 1.405 | -1.85 |
| 60 | | 10.91 | 34.72 | 17.44 | .080 | 1.09 | 2498 | .830 | 8.84 | 7,469 | 1.94 | 5.82 | .550 | .29 | 2.409 | 1.776 | -1.45 |

[a]Average of four repeat impacts.

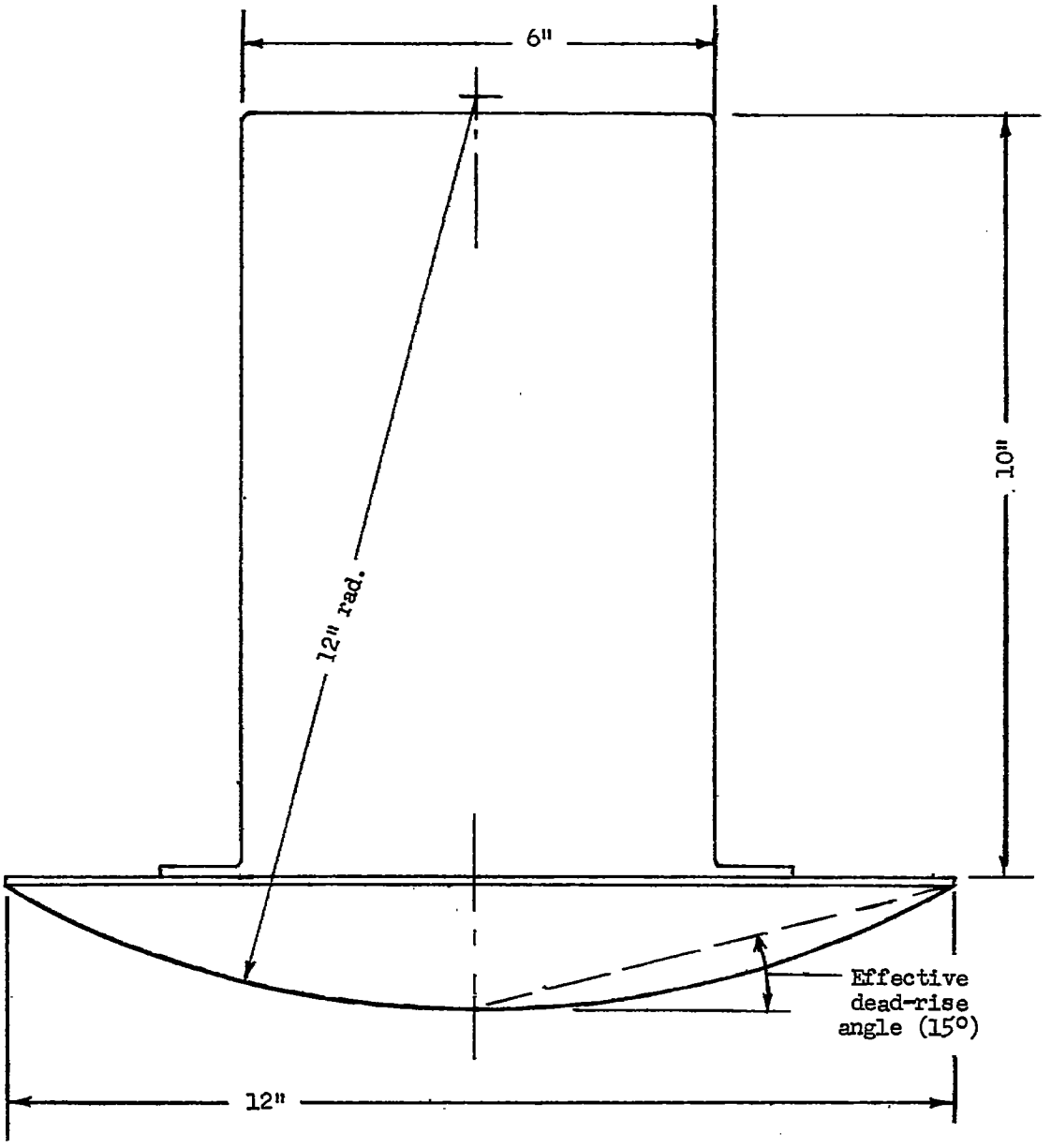


Figure 1.- Cross section of circular-arc model.

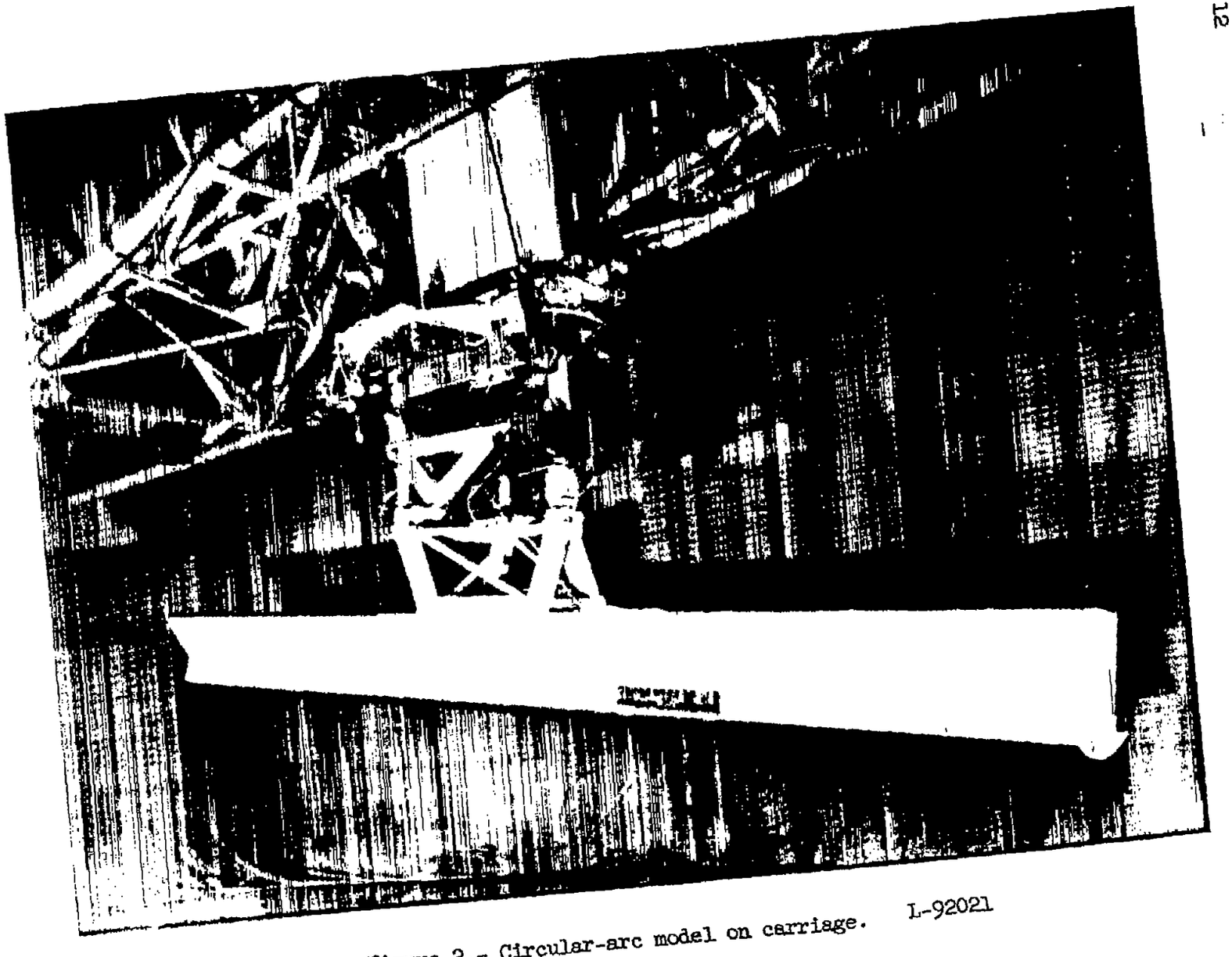

Figure 2.- Circular-arc model on carriage. L-92021

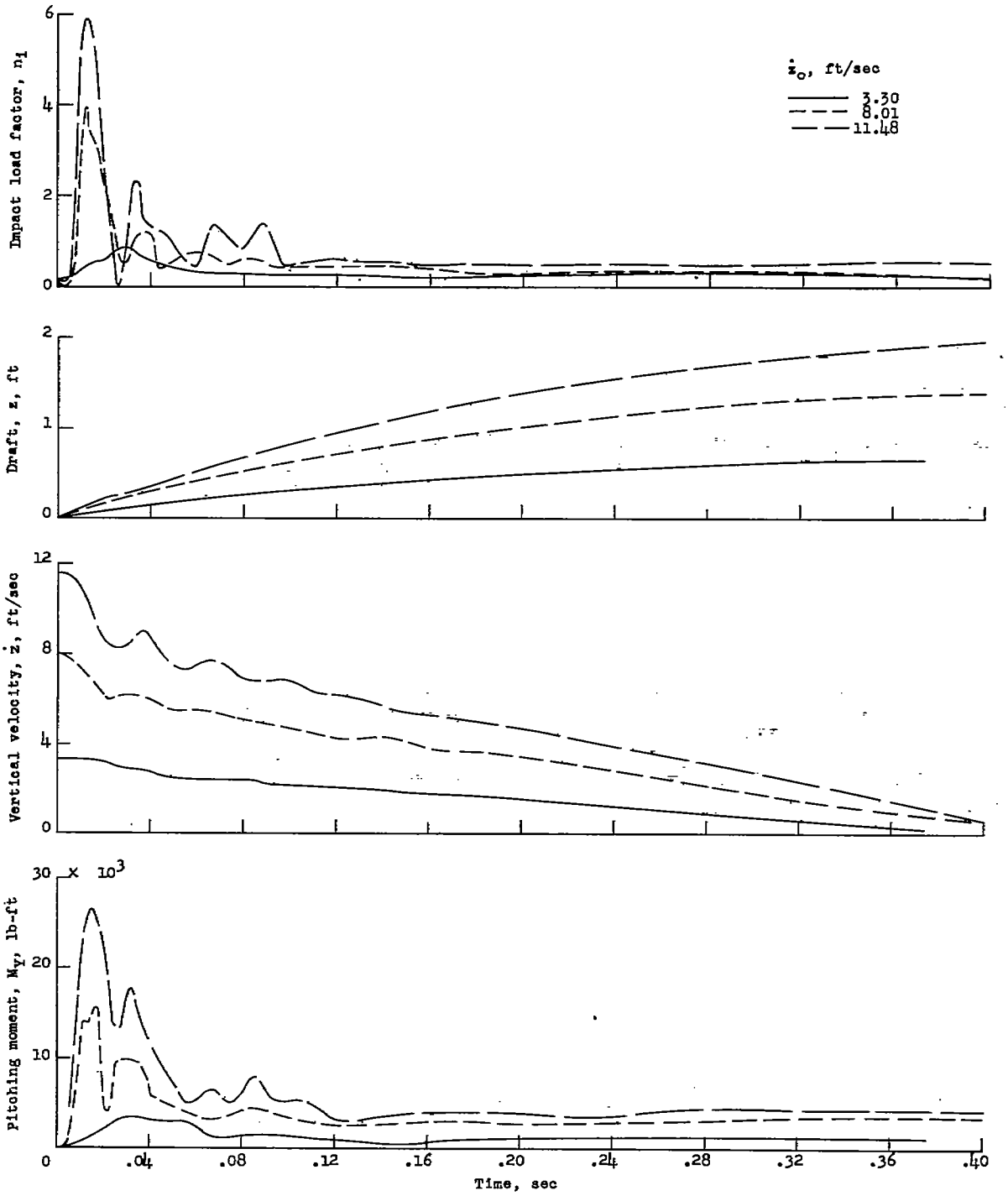


Figure 3.- Sample time histories of loads and motions from vertical-drop tests without forward speed. $\tau = 0^\circ$; $C_\Delta = 18.59$.

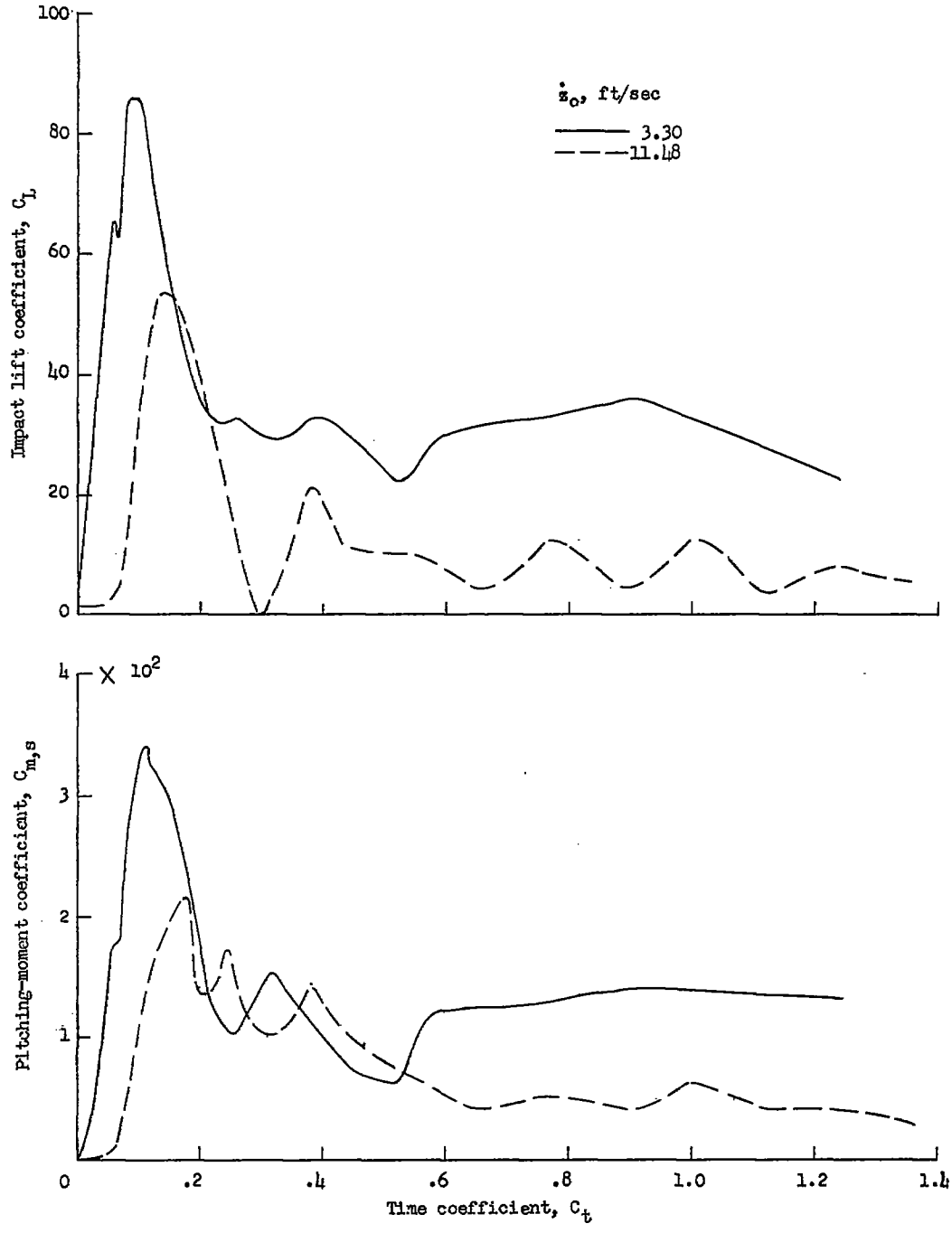


Figure 4.- Sample variations of lift and pitching-moment coefficients with time coefficient for vertical-drop tests without forward speed. $\tau = 0^o$; $C_\Delta = 18.59$.

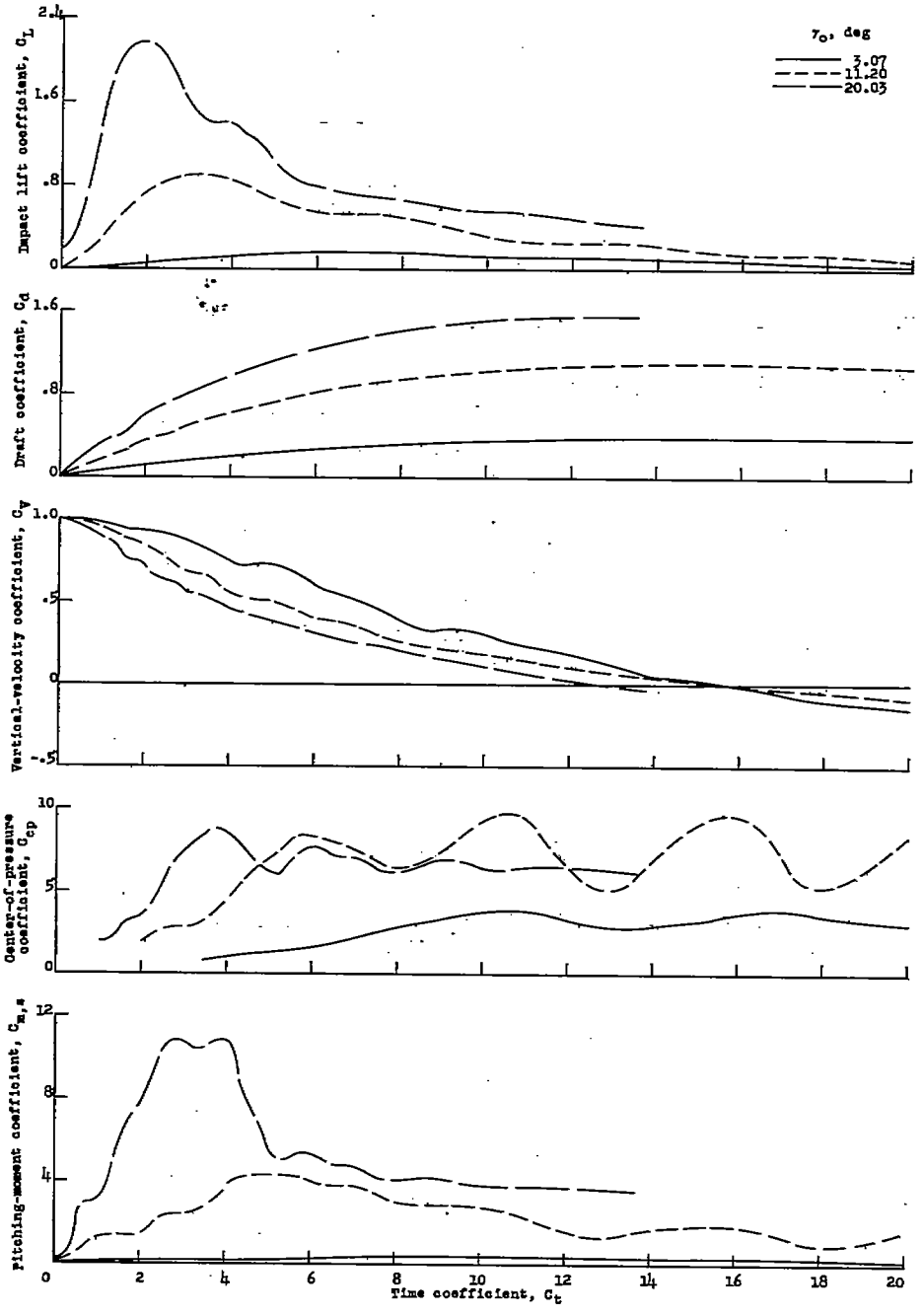


(a) $\tau = 4^o$.

Figure 5.- Variations of coefficients with time coefficient for impacts with forward speed. $C_\Delta = 18.59$.

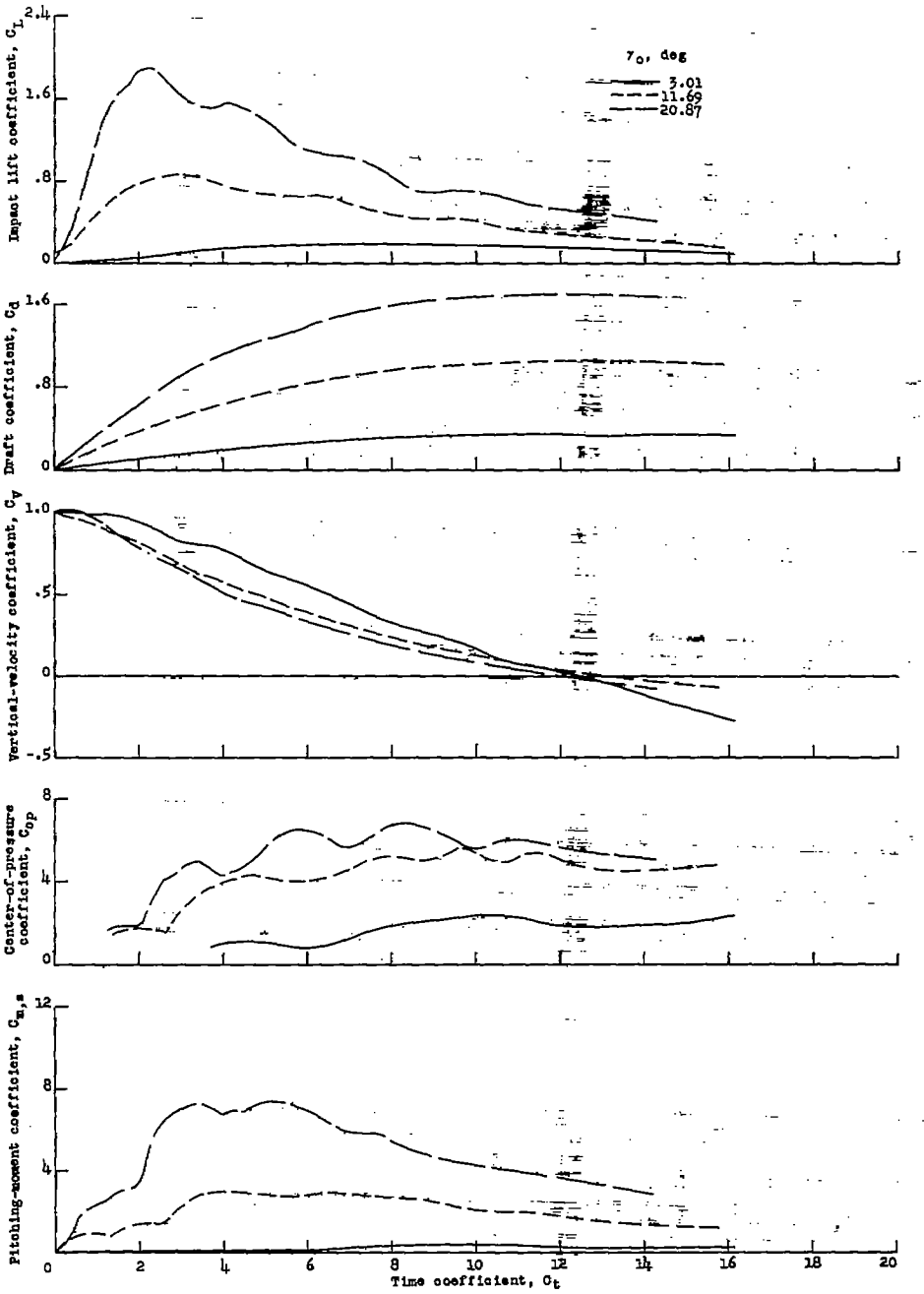


(b) $\tau = 8^{\circ}$.

Figure 5.- Continued.

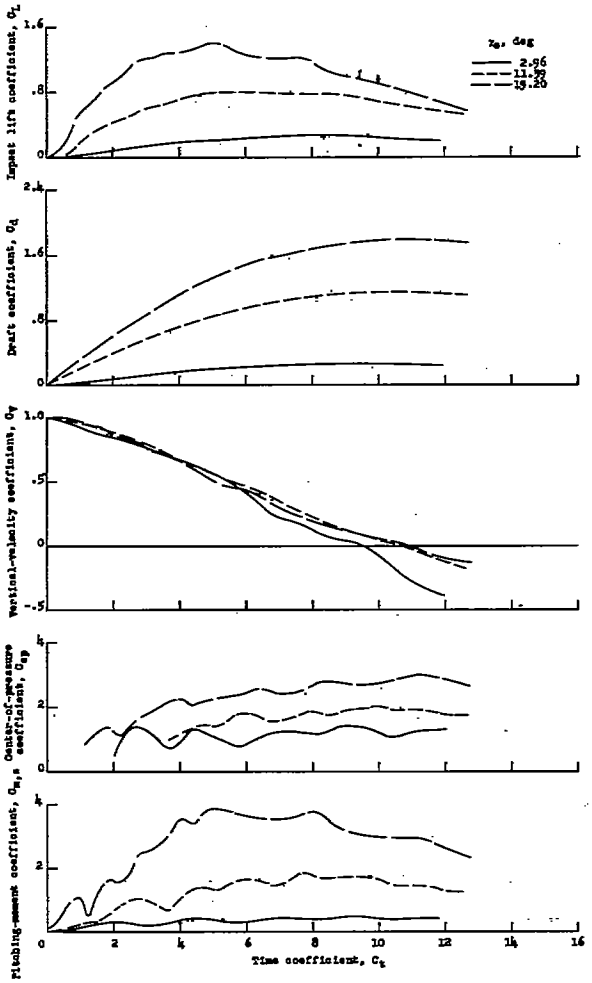


(c) $\tau = 30^\circ$.

Figure 5.- Concluded.

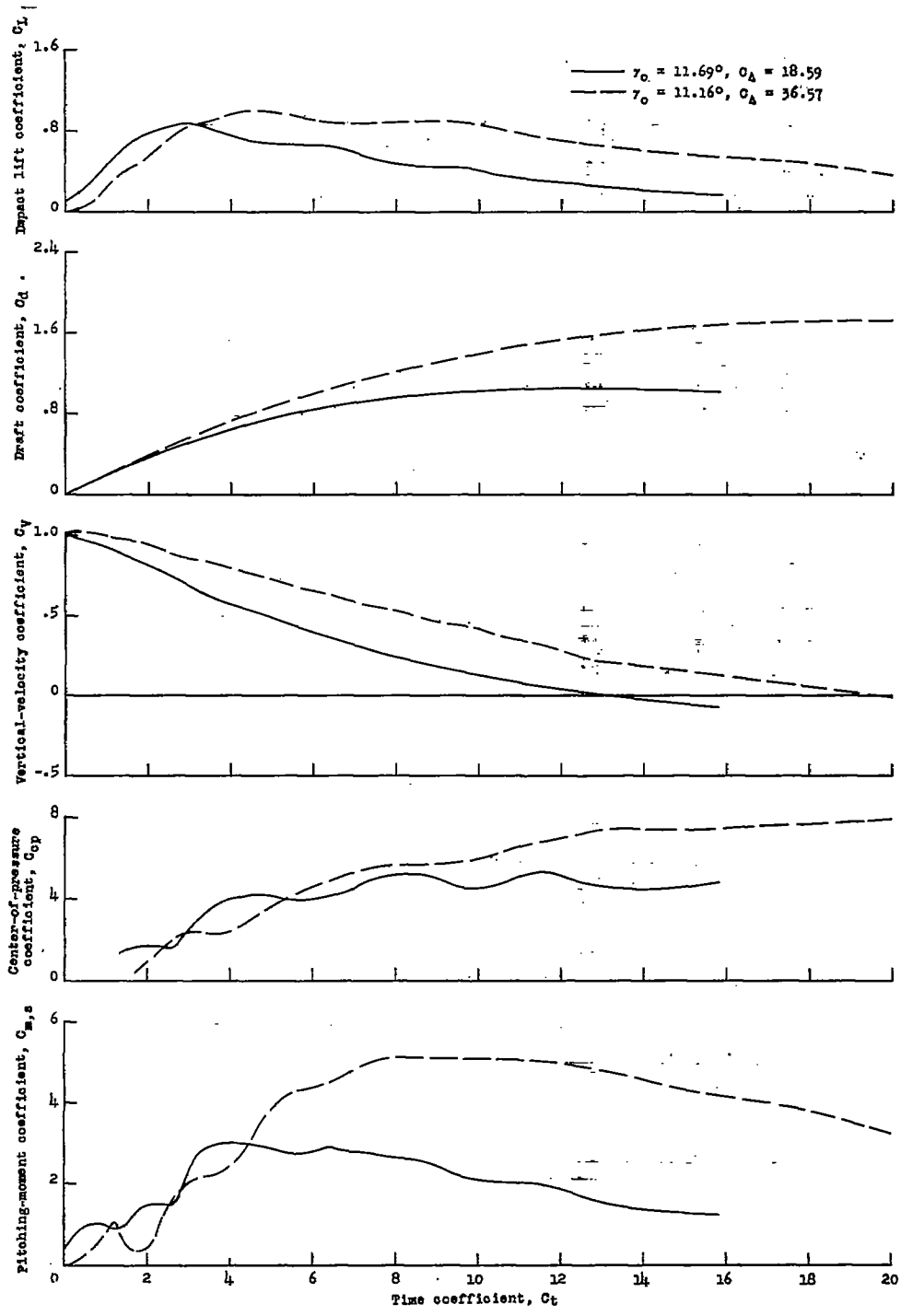


Figure 6.- Time histories of coefficients from impacts with forward speed. $\tau$ = 8°; $C_\Delta$ = 18.59 and 36.57.

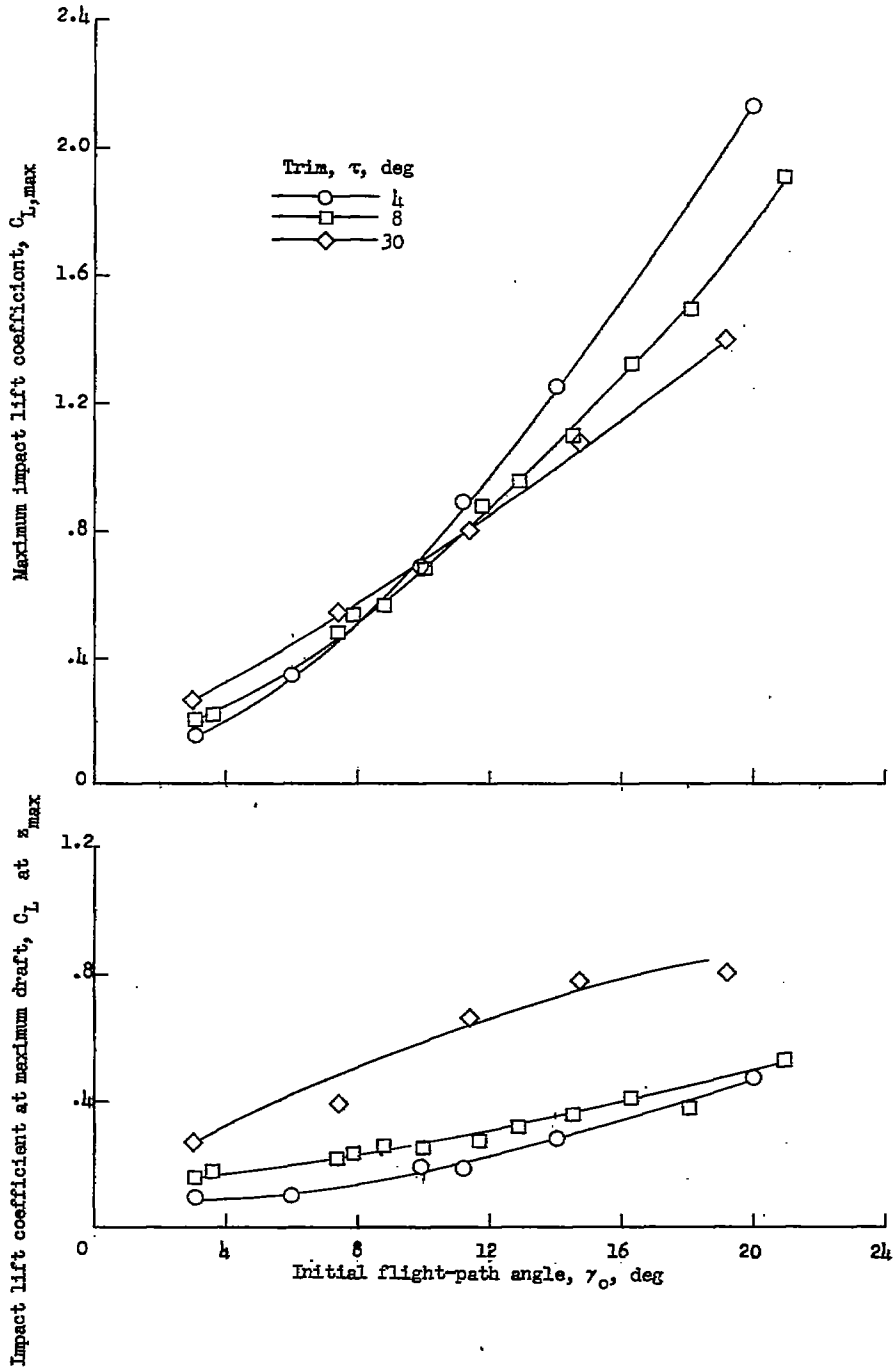


(a) Impact lift coefficient, $C_L$.

Figure 7.- Variations of coefficients with initial flight-path angle. $C_\Delta = 18.59$.

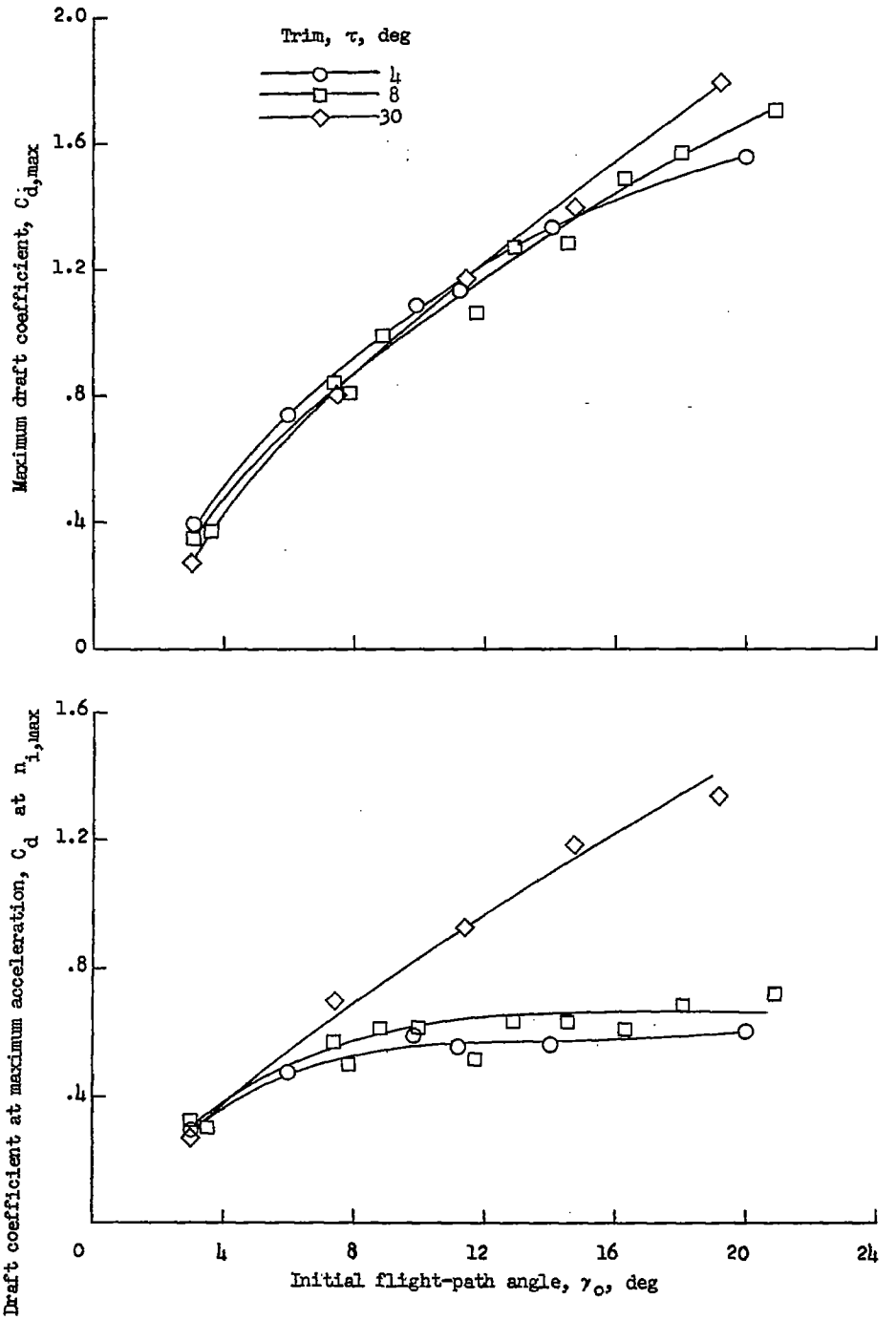


(b) Draft coefficient, $C_d$.

Figure 7.- Continued.

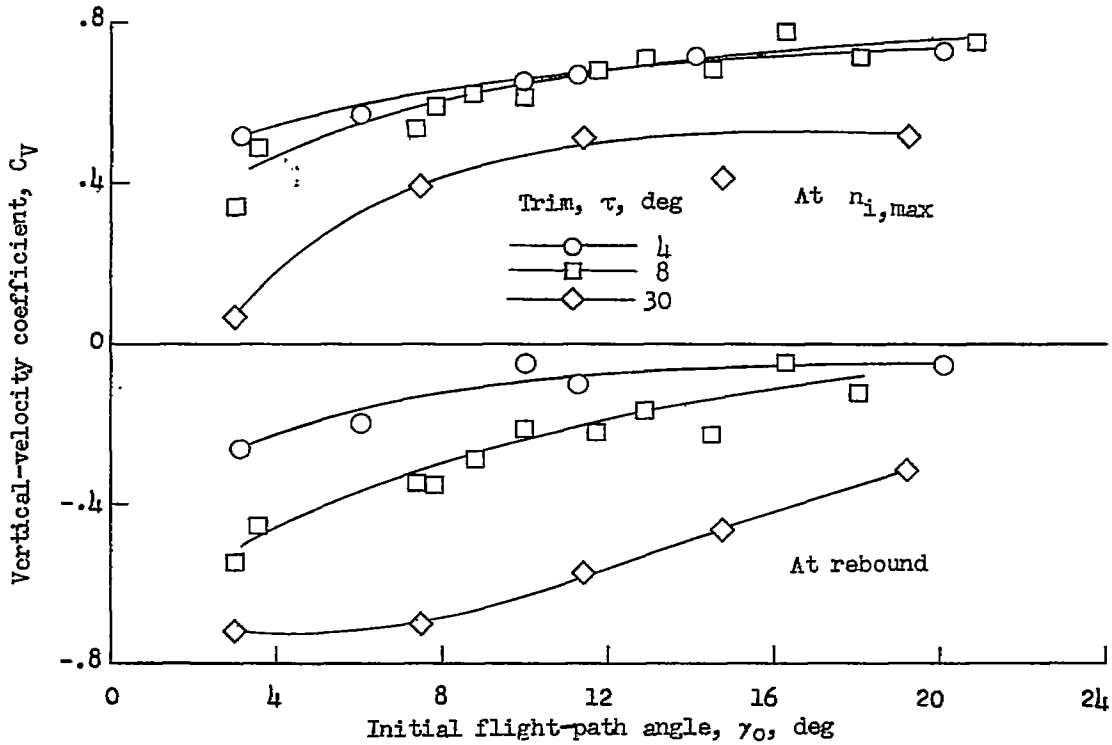


(c) Vertical-velocity coefficient, $C_V$.

Figure 7.- Continued.

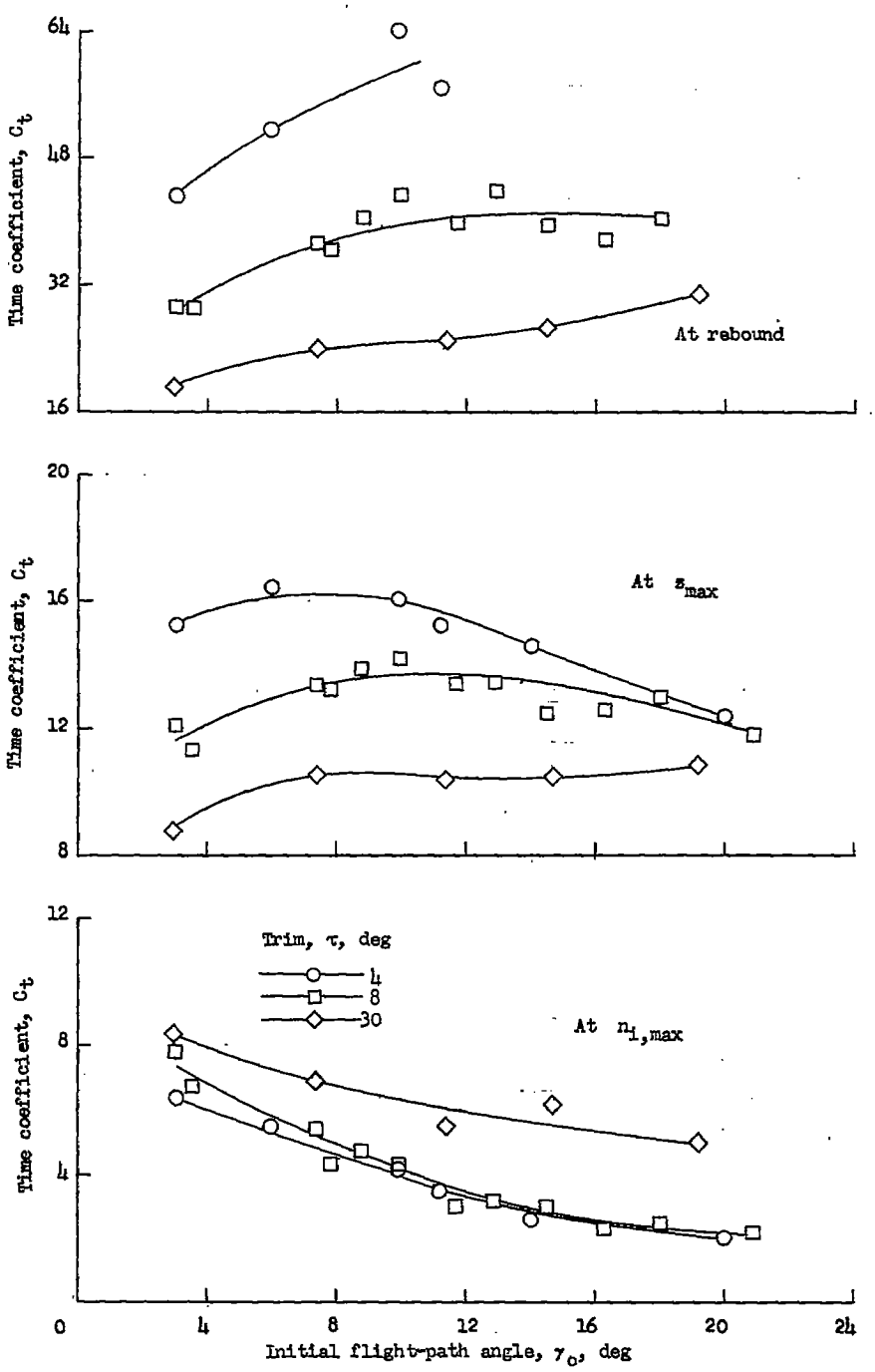


(d) Time coefficient, $C_t$.

Figure 7.- Continued.

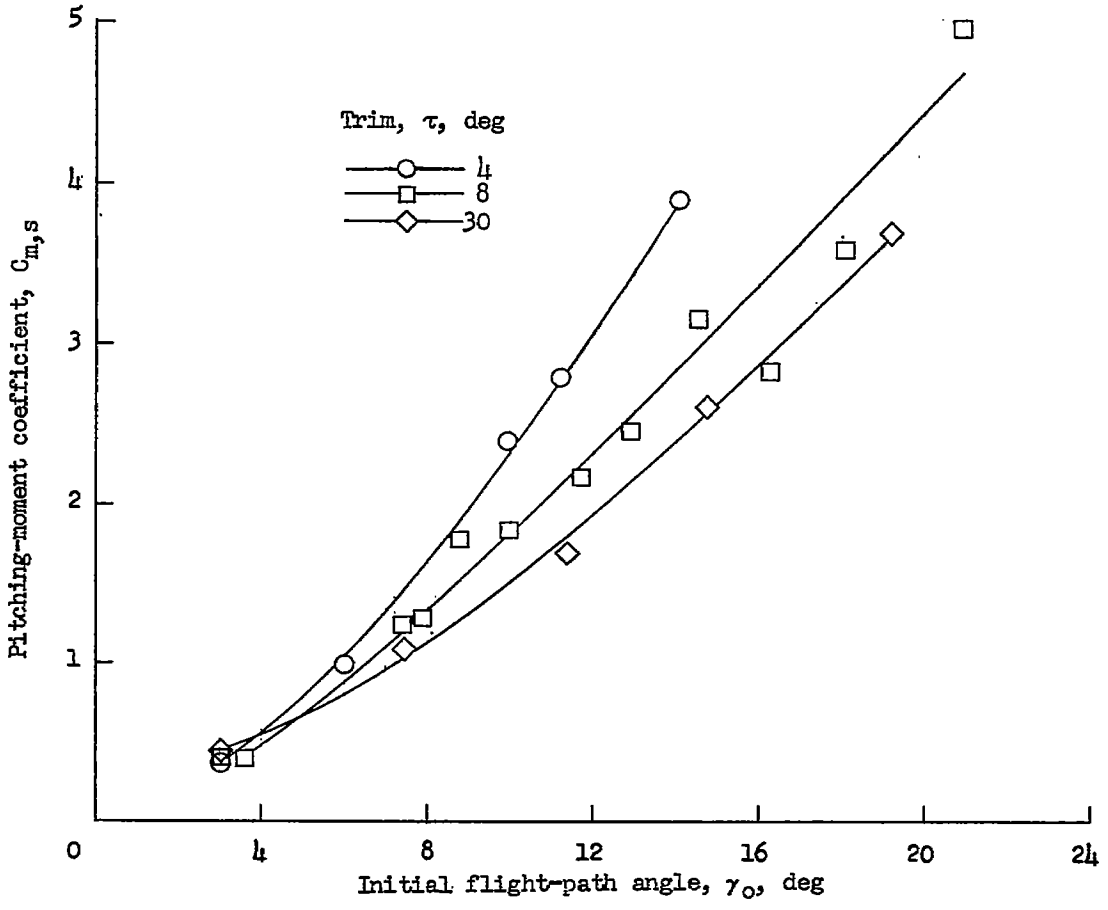


(e) Pitching-moment coefficient, $C_{m,s}$.

Figure 7.- Continued.

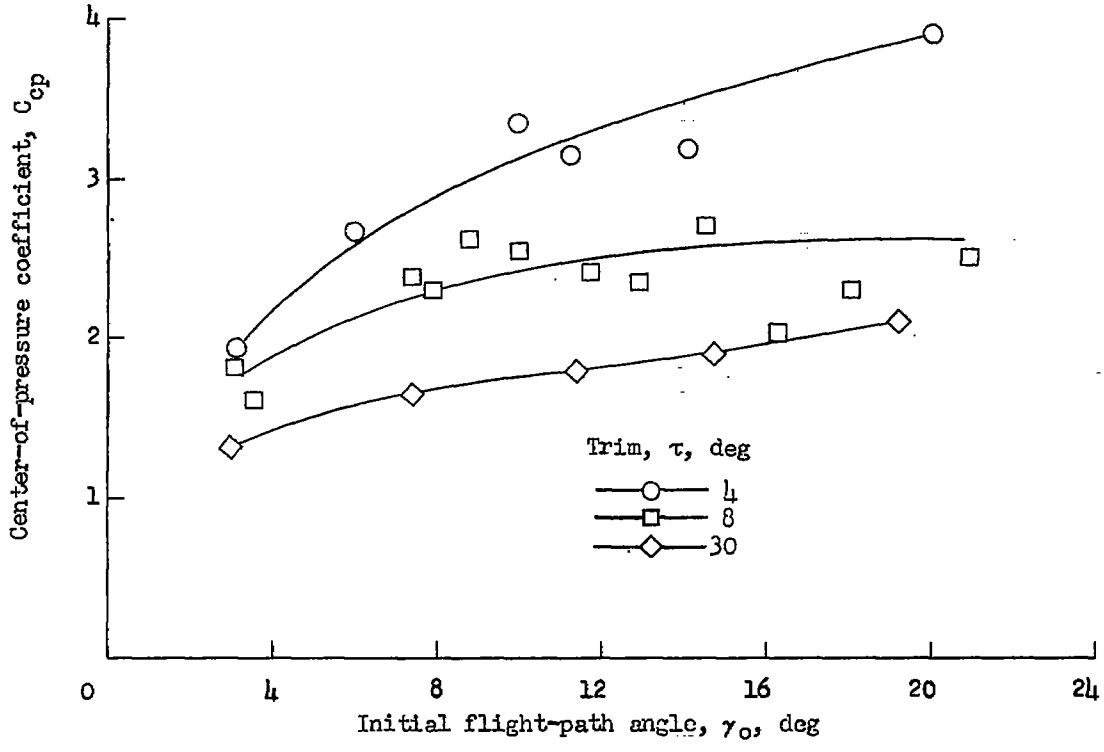


(f) Center-of-pressure coefficient, $C_{cp}$.

Figure 7.- Concluded.

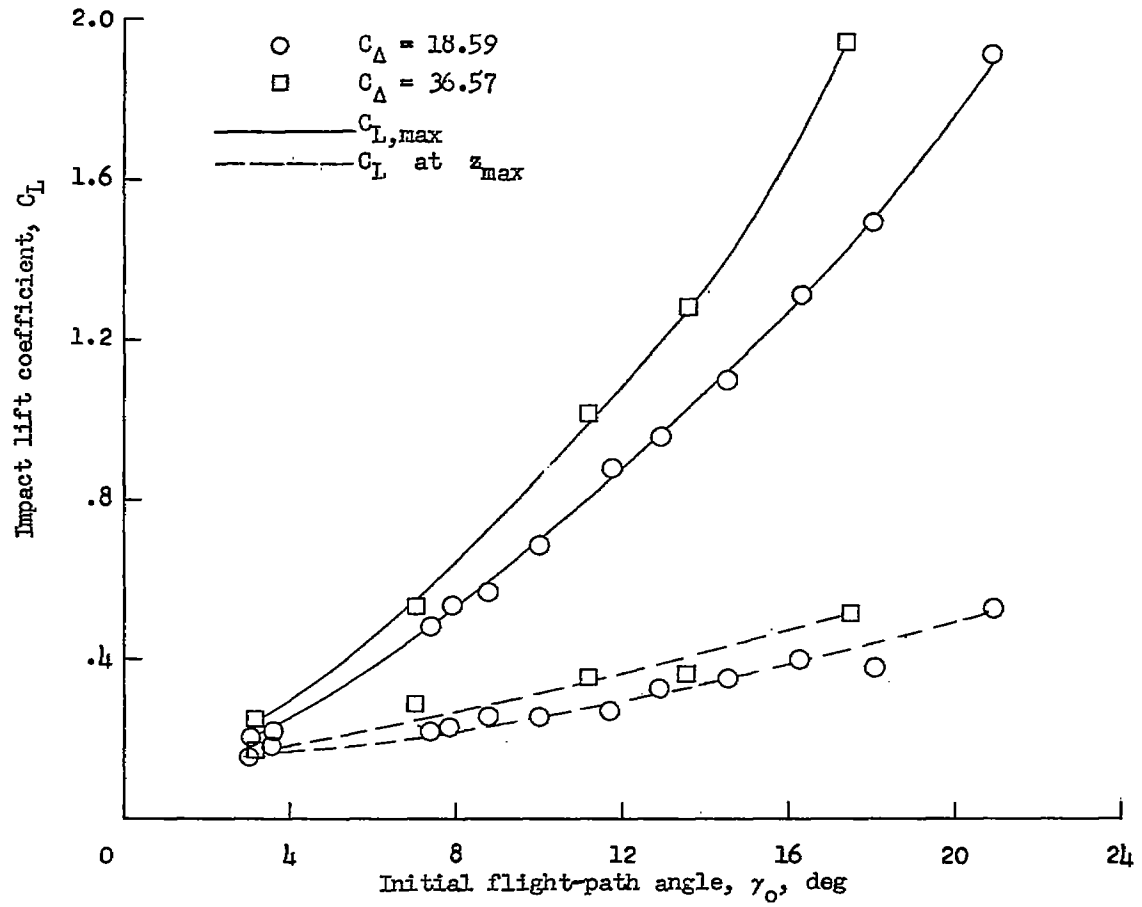


(a) Impact-lift coefficient, $C_L$.

Figure 8.- Variations of coefficients with initial flight-path angle. $\tau = 8°$; $C_\Delta = 18.59$ and 36.57.

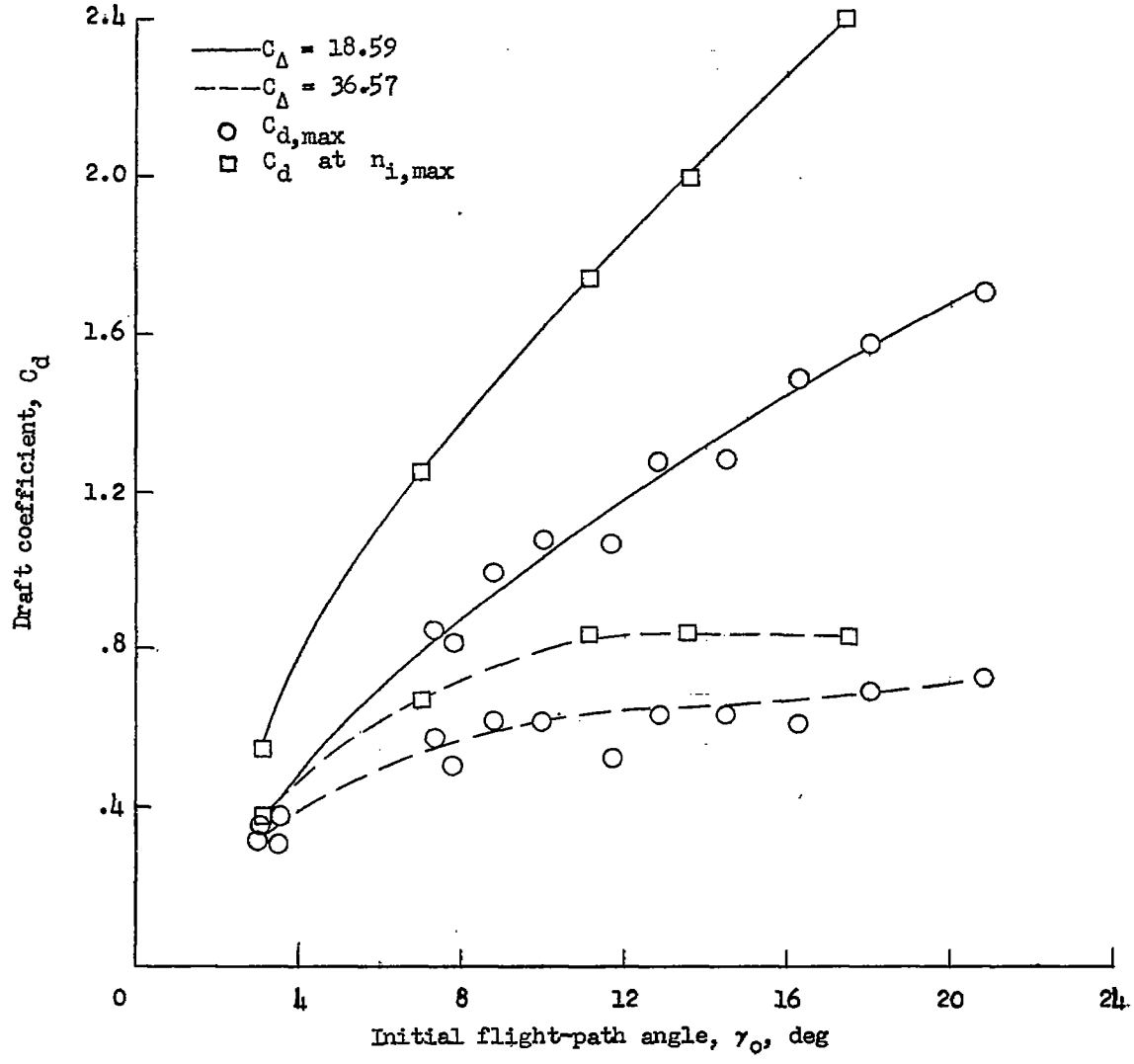


(b) Draft coefficient, $C_d$.

Figure 8.- Continued.

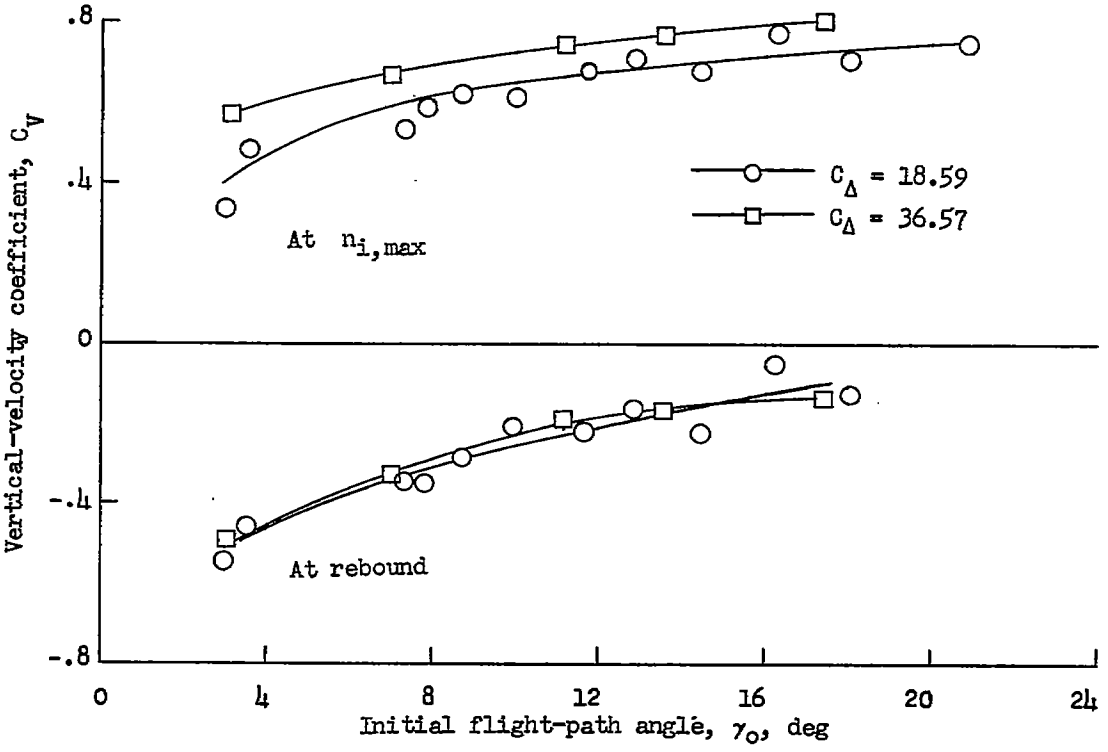


(c) Vertical-velocity coefficient, $C_V$.

Figure 8.- Continued.

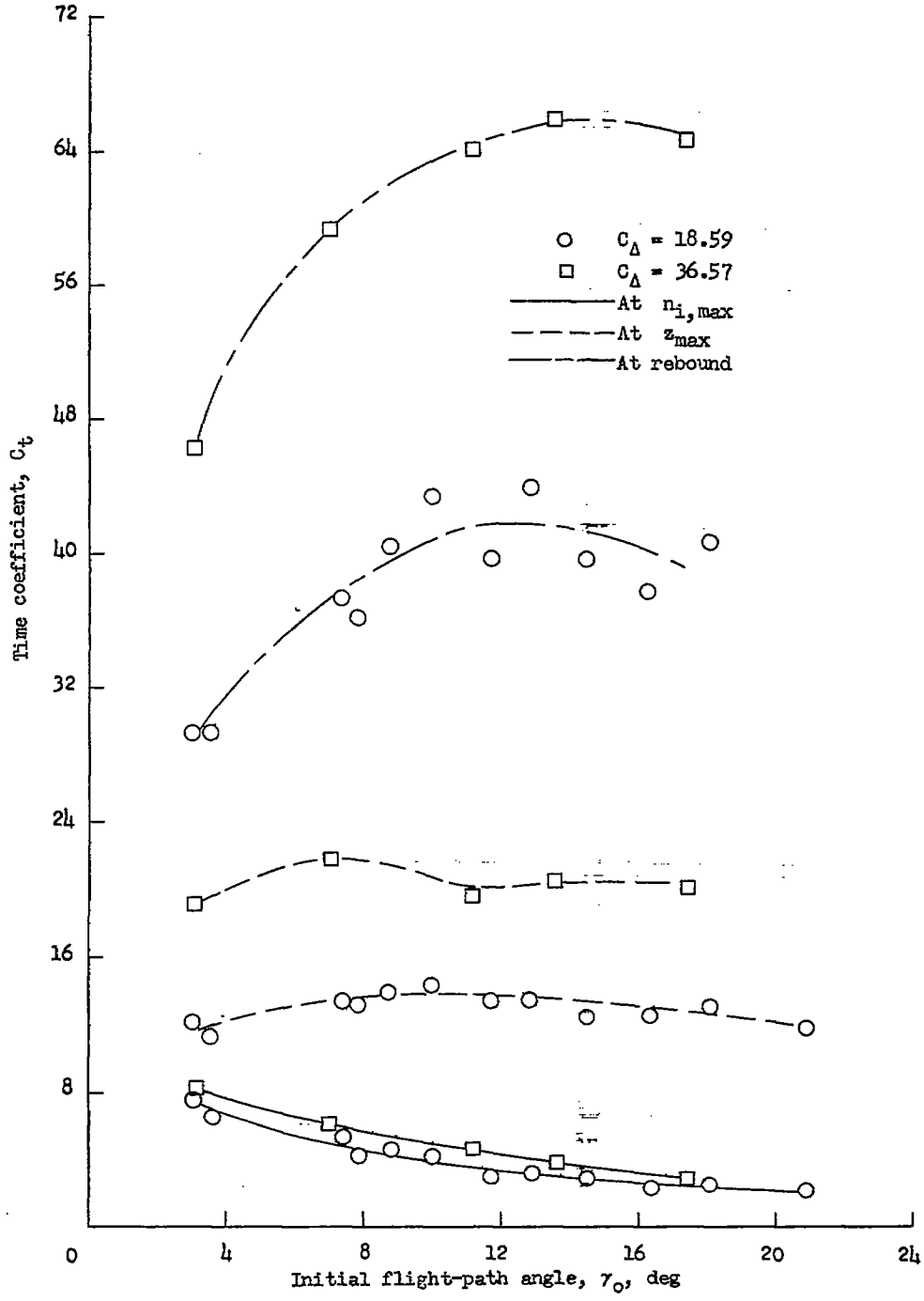


(d) Time coefficient, $C_t$.

Figure 8.- Continued.

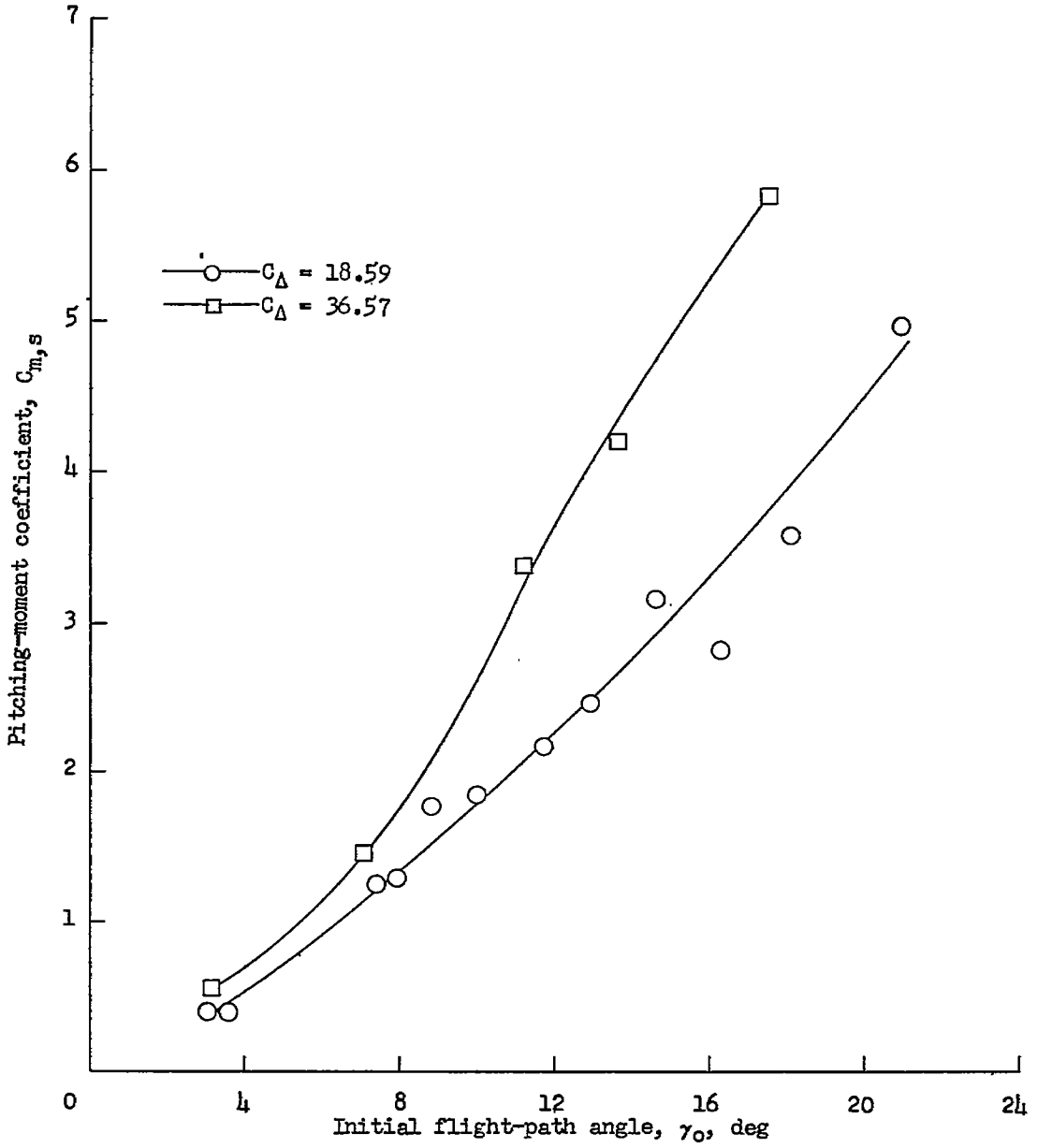


(e) Pitching-moment coefficient, $C_{m,s}$.

Figure 8.- Continued.

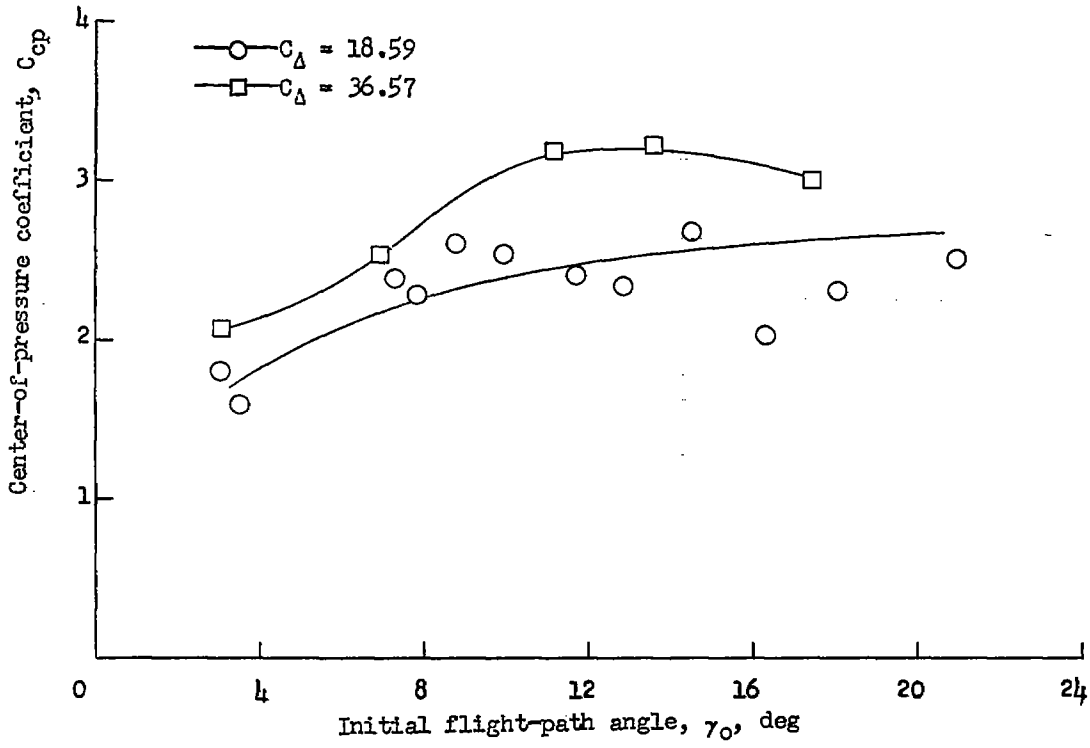


(f) Center-of-pressure coefficient, $C_{cp}$.

Figure 8.- Concluded.

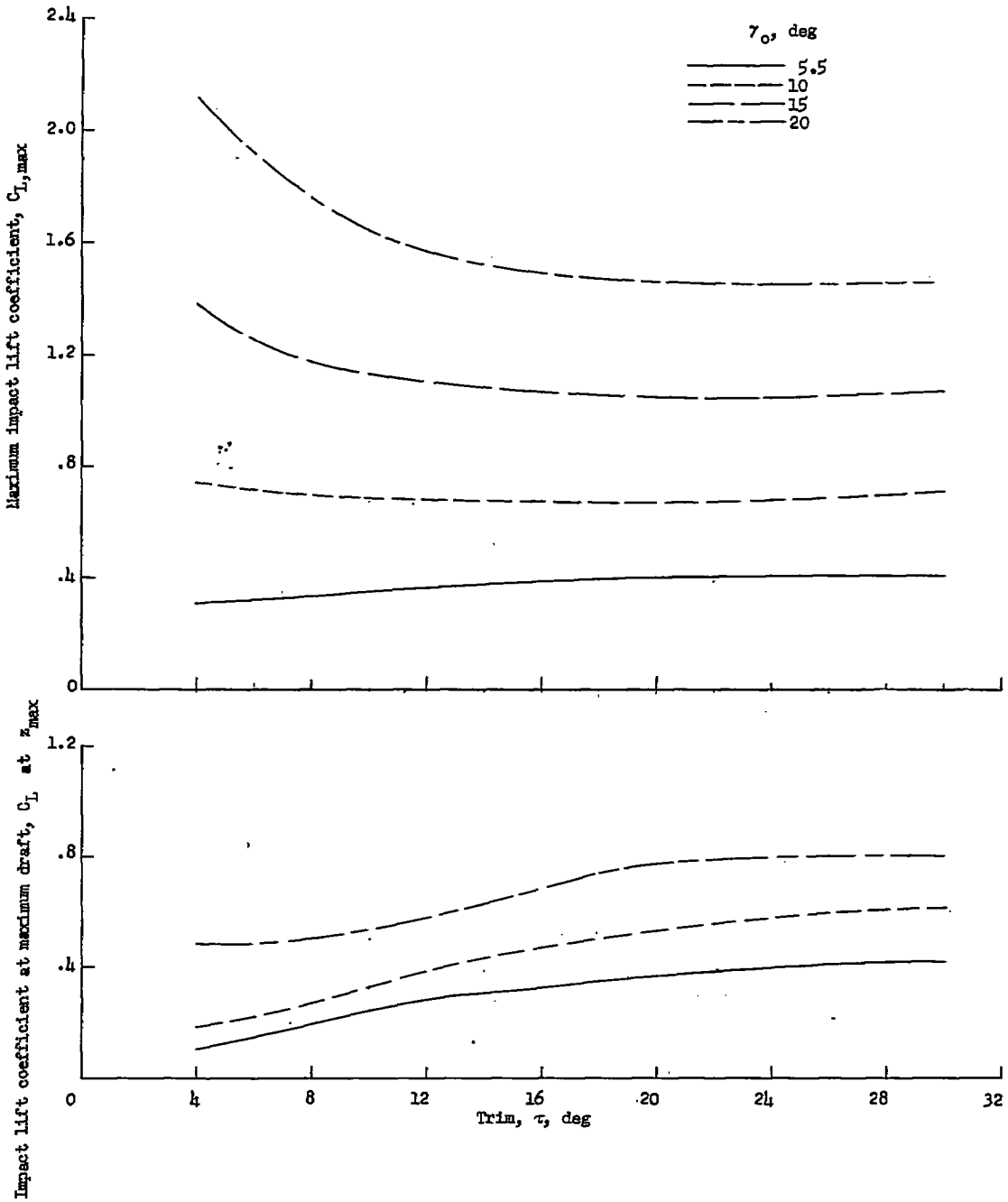


(a) Impact lift coefficient, $C_L$.

Figure 9.- Variations of faired values of coefficients with angle of trim for several initial flight-path angles. $C_\Delta = 18.59$.

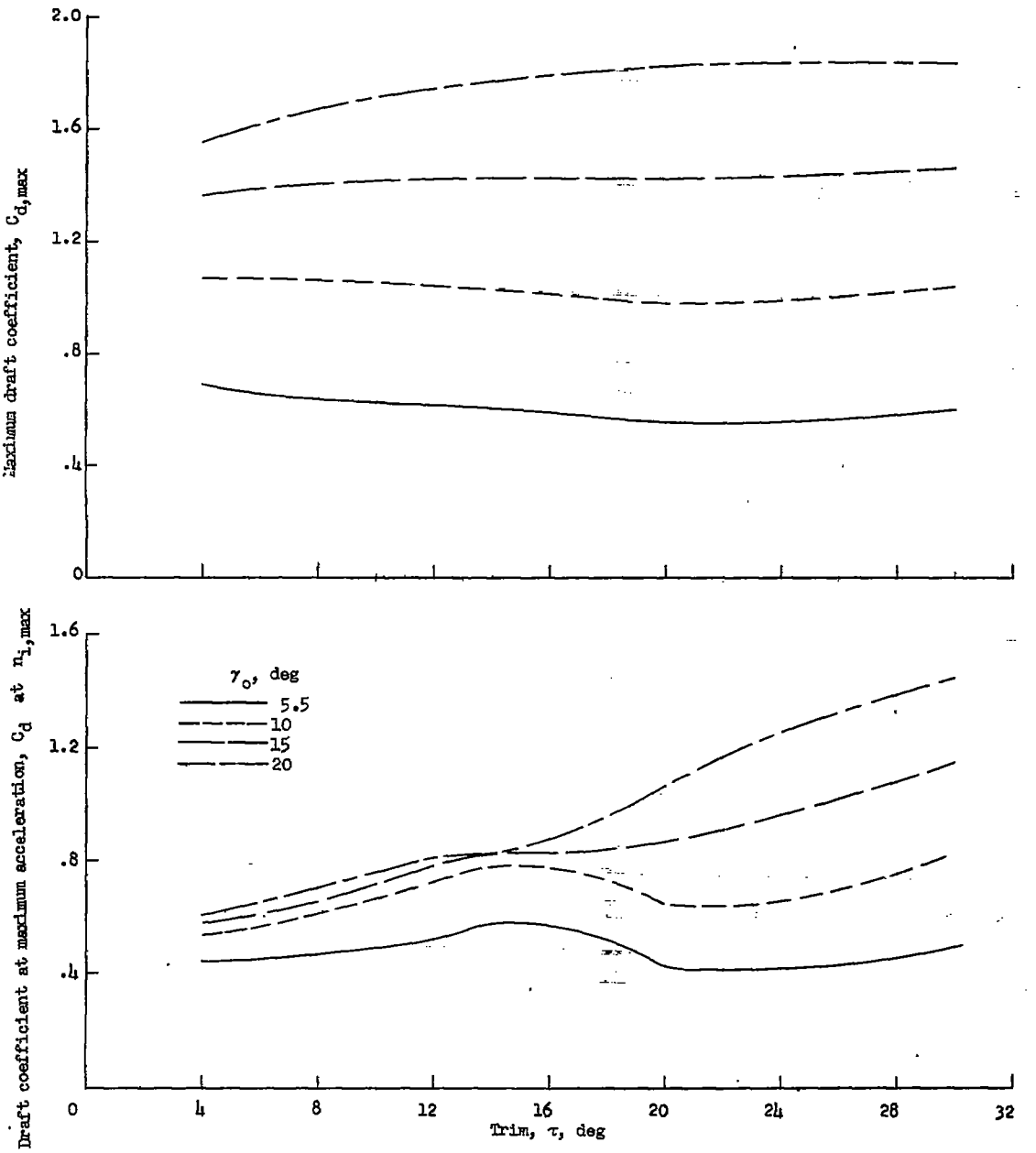


(b) Draft coefficient, $C_d$.

Figure 9.- Concluded.

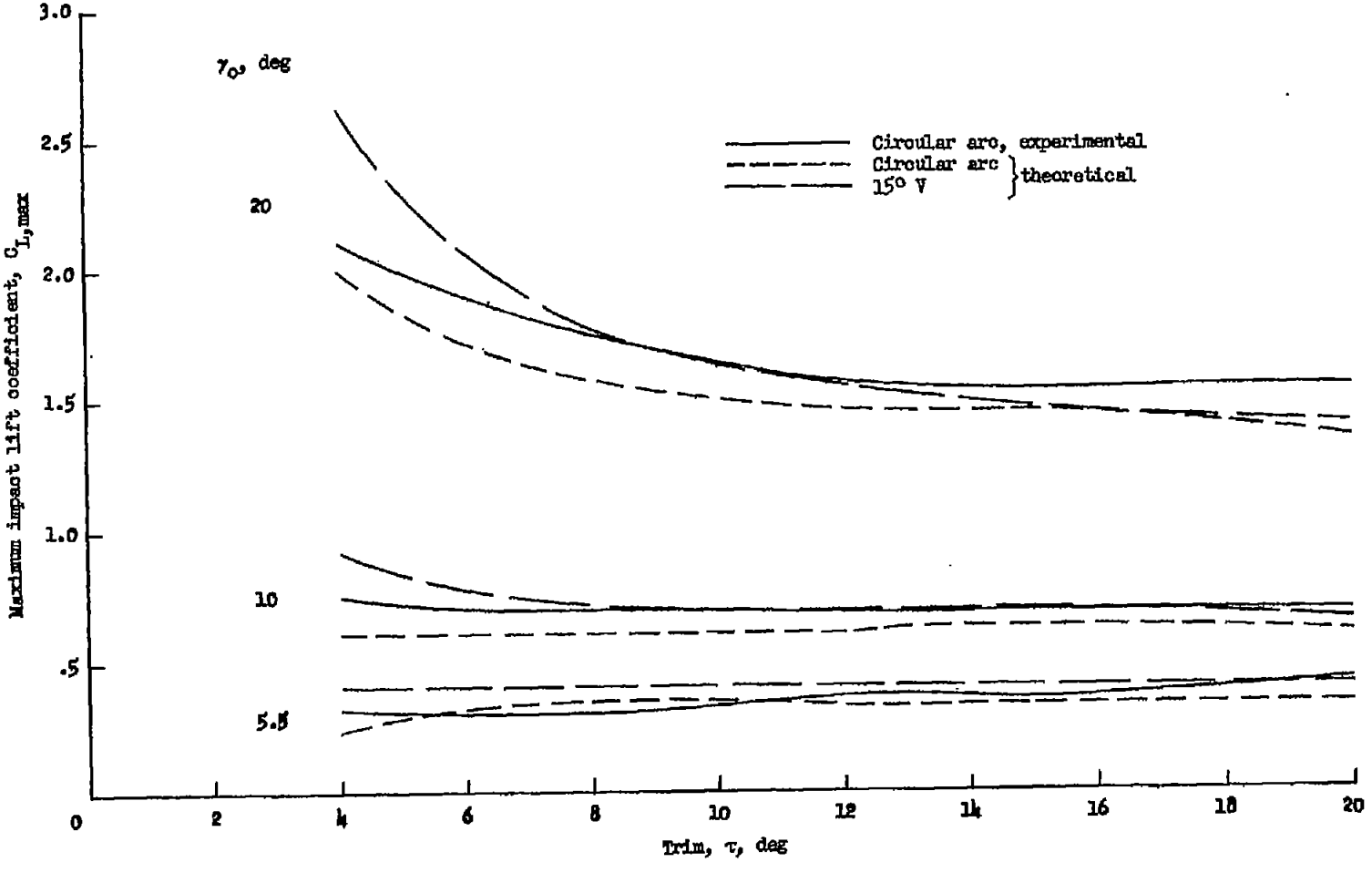


Figure 10.- Comparisons of maximum lift coefficients for circular-arc and V-bottom models. $C_\Delta = 18.59$.

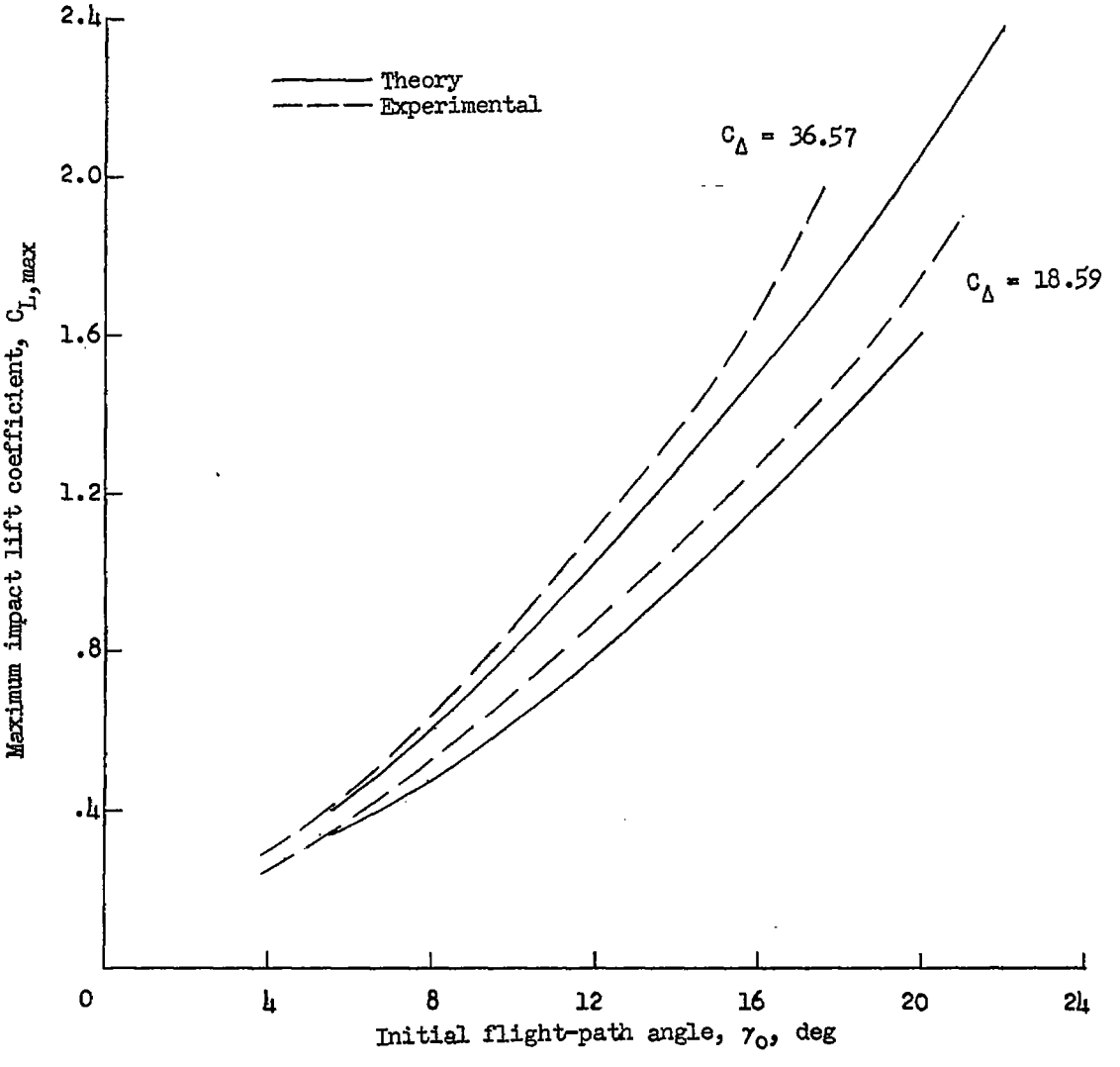


Figure 11.- Comparisons of theoretical and experimental lift coefficients for circular-arc model. $\tau = 8^\circ$; $C_\Delta = 18.59$ and 36.57.

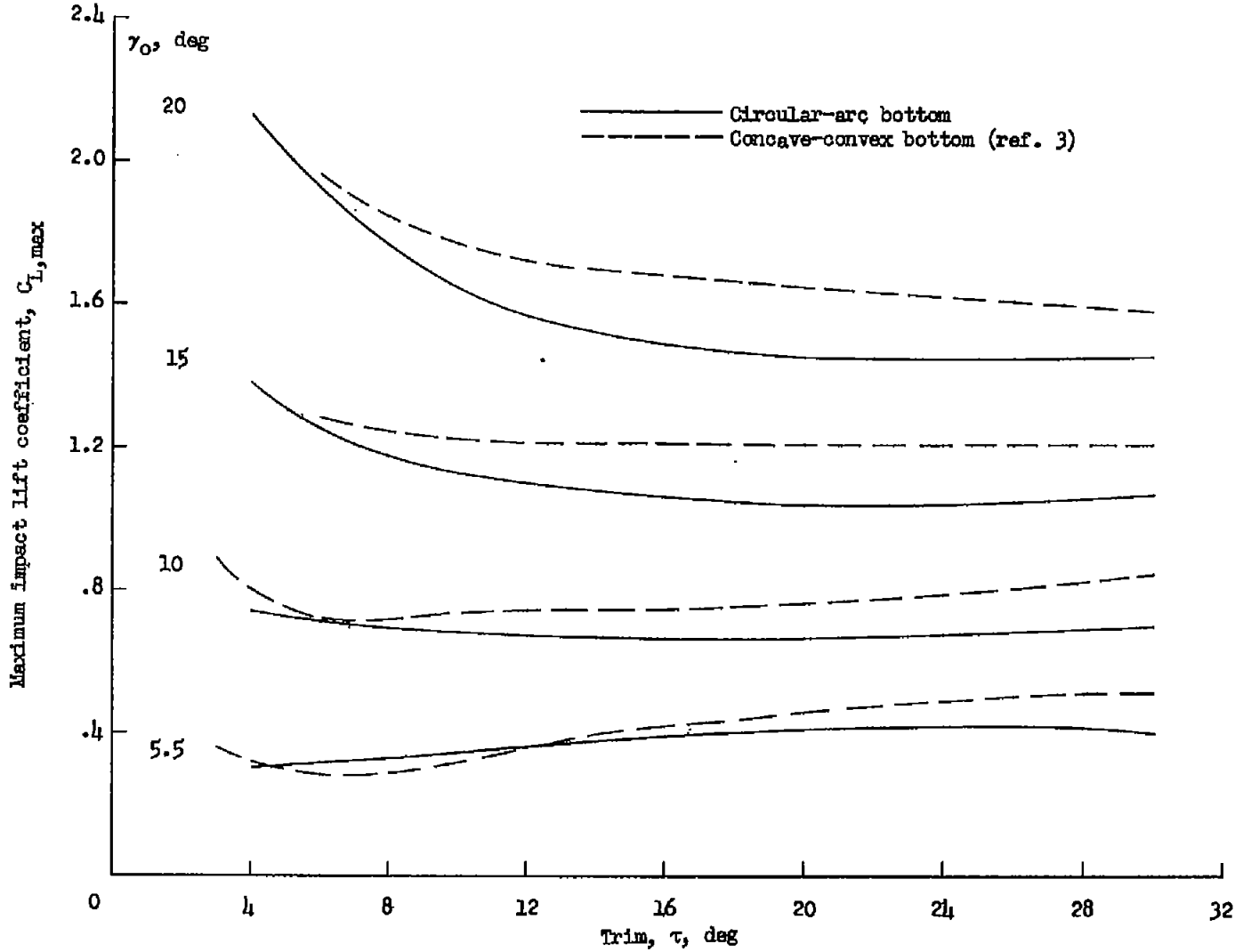


Figure 12.- Comparison of variations of maximum lift coefficient with trim for the circular-arc and concave-convex bottoms.